An experimental study on atmospheric diffusion

By ULF HÖGSTRÖM, *The Swedish Meteorological and Hydrological Institute, Stockholm*

(Manuscript received October 9, 1963)

ABSTRACT

A method has been devised by which atmospheric diffusion can be studied over a few kilometres range with rather good precision at only moderate expense. The method which is based on smoke puff photography is especially well suited for thermally stable conditions. It is possible to study the effect of both the low frequency part and the high frequency part of the Lagrangian spectrum of turbulence on the diffusion. More than 100 complete experiments have been performed at two places in Sweden at three different levels of release.

The vertical standard deviation of matter is found to be a function of the following stability parameter: $(\partial\theta/\partial z)/u_f^2$, where $\partial\theta/\partial z$ is the local vertical gradient of potential temperature, and u_f is "the free wind", that is the wind just above the friction layer. A comprehensive formula, or rather a system of formulae, for the variation of the vertical standard deviation (sampling time about one hour) with distance from the source, stability and height above the ground of the point of release, has been developed. The formulae are believed to have a very general application, the only site parameter being necessary to know is the roughness length, z_0. The formulae have been successfully tested against results from various tracer experiments described in the literature.

The variance of the horizontal distribution of matter for one hour sampling time is found to be the sum of two parts: one which is independent of stability and one which is dependent on stability in much the same way as is the vertical variance.

The distribution of matter from a ground level release is described by new formulae. The result is in good agreement with experimental and theoretical evidence in the literature.

Introduction

In Studsvik and Ågesta, both places situated less than 100 kilometres from Stockholm, Sweden built its first two atomic energy establishments of appreciable size during the fifties and early sixties. As these projects are to a great extent of an investigative character, an extensive program for studying atmospheric dispersion and "dispersion climatology" at the two places was adopted also.

The program adopted was realized in cooperation between AB Atomenergi and the Swedish Meteorological and Hydrological Institute during the years 1960–1963. The investigation was defrayed by AB Atomenergi.

At both Studsvik and Ågesta continuous measurements of wind and temperature were performed on a mast, 120 m high and besides at several minor stations up to some kilometres distance from the main stations.

An extensive program for investigating the atmospheric dispersion experimentally, especially for stable stratification, was planned and performed. It is the result of these investigations that is now presented.

The report is divided into five separate parts. In part I the experimental method used is presented. Further an account of the experimental results is given with special emphasis on the influence of stability.

In part II the experimental results found are analysed further in the light of existing theories to give a general formula for dispersion from an elevated source as a function of stability and of source height above the ground.

In part III a general formula for ground level release is proposed. The formula is tested thoroughly against experimental data from this investigation and from investigations to be found in the literature.

In part IV is described how the dispersion pattern is modified by the presence of a topographical discontinuity at one of the two experimental sites, Studsvik.

In part V the effect of wind direction shear on the diffusion is discussed theoretically.

Part I. A new photographic method for investigating atmospheric diffusion over a few kilometres range

1. Description of the method

The most direct way of studying atmospheric diffusion consists in releasing some suitable tracer which is then collected at several points in the surroundings of the source. To yield sufficiently detailed information the sampling net-work must be rather dense—the "Project Prairie Grass" (BARAD & HAUGEN, 1958) and the "Green Glow Diffusion Program" (BARAD & FUQUAY, 1962) illustrate this point clearly. This renders it very expensive to make systematic investigations with tracer techniques, such systematic investigations being necessary when studying the influence of thermal stability, height above the ground etc. upon atmospheric diffusion.

From what is said above, it is easily understood that many indirect methods for studying atmospheric diffusion have been developed. These usually consist in taking photographs of continuously emitted smoke or of smoke puffs. ROBERTS (1923) seems to have been the first to try this way. He put forward an "opacity theory" according to which one can "see" a dark smoke cloud against a brighter background provided there is an integrated particle density in the line of sight greater than some threshold value. This is the starting point of all subsequent studies of this type. ROBERTS further assumed constant eddy diffusivity, an assumption which is generally not acceptable. ROBERTS' successors, for instance SUTTON (1932), FRENKIEL & KATZ (1956) and KELLOGG (1956), rejected this assumption but introduced other specified assumptions concerning the eddy diffusivity. In 1957 GIFFORD (1957) showed that from smoke puff photographs it is possible to evaluate how the particle standard deviation relative to the puff centre varies with time without making any other assumptions about the diffusion than that the particles are normally distributed within the cloud. As will be discussed later, this assumption is very well supported by observations.

In most studies instantaneous smoke puffs have been used. This means that the diffusion can only be studied over a very limited time —mostly less than one minute—simply because the smoke disappears so rapidly. In the investigation now to be presented it has been possible to extend the time over which the cloud can be effectively observed to more than an hour in extreme stable conditions and to about ten minutes in neutral conditions. This is accomplished by a combination of two means: firstly the cloud is generated by continuous emission over a finite time interval, 30 seconds in duration, secondly the cloud is viewed from the very point of release in the direction of travel, so that the smoke particles released over 30 seconds superimpose to produce high integrated concentrations in the line of sight. The cloud is produced by a Swedish army smoke generator and consists of oil drops, fairly uniform in diameter: 0.6 μ. A 30 seconds-cloud is estimated to contain about 10^{15} drops. When the cloud is viewed from behind as here, it is possible to study simultaneously the diffusion in the vertical (z-direction) and in the horizontal crosswind direction (y-direction). In previous studies the puffs seem always to have been viewed in a direction perpendicular to the line of travel so that either the z-diffusion or the y-diffusion could be studied but not both at a time.

Before going into details concerning the evaluation of the smoke puff photographs, we will inquire how to interpret the results broadly. In two outstanding papers, BATCHELOR (1949) and (1952) has elucidated the outstanding difference of diffusion in a fixed coordinate system and diffusion relative to a system the origin of which is fixed to the centre of gravity of a moving cloud. In the fixed system type diffusion (BATCHELOR, 1949) all wave numbers of the turbulent motion are effective in dispersing the cloud near the source. With increasing distance from the source the high-frequency osciallations gradually loose importance, so that eventually only the very low wave numbers contribute to further dispersion. In relative diffusion (BATCHELOR, 1952) on the other hand, those eddies which are less than the dimensions of the cloud, are dominant in dispersing it. But as the dispersion goes on the cloud grows so that lower and lower wave numbers are brought into action. In this way relative diffusion becomes an accelerating process in the earlier stages. This is especially evident in the case of an instantaneously generated cloud. When the dimensions of the cloud are less than the upper wavelength limit of the inertial subrange but greater than the microscale of turbulence, $\nu^{\frac{3}{4}}\varepsilon^{-\frac{1}{4}}$, ($\nu$ being the kinematic viscosity and ε the energy dissipation) then the standard deviation of the particles relative to the cloud centre increase with time as $t^{\frac{3}{2}}$. This contrasts to fixed system type diffusion where the standard deviation never grows faster than t (in quasi-homogeneous turbulence of which we speak all the time). GIFFORD's (1957) reexamination of the smoke puff experiments of KELLOGG and of FRENKIEL & KATZ clearly shows the existence of the $t^{\frac{3}{2}}$-region for atmospheric diffusion.

We now turn to the smoke experiments of our present study. If we fix a coordinate system to a moving puff, and evaluate the spread of smoke in this system, we clearly have to do with relative diffusion. But already from the beginning the cloud which has been generated over 30 seconds has the length $30 \cdot \bar{u}$, where $\bar{u}$ is the mean wind speed at the level of release. This means that all eddies with wavelengths less than about $30 \cdot \bar{u}$ are effective in diffusing the cloud relative to its moving centre. As time goes on the cloud will of course grow, but it will take a fairly long time before it has been, say doubled in length and this is especially pronounced when the diffusion is slow, that is in inversion conditions. In this way the relative diffusion will be governed by a rather large part of the spectrum, the low wave number limit of which will be displaced only slowly towards lower numbers. Because the isotropic limit in the atmospheric surface layer is at wavelengths comparable to the height above ground (see for instance BATCHELOR, 1950, and PRIESTLEY, 1959), which is in most cases less than $30 \cdot \bar{u}$, the $t^{\frac{3}{2}}$-law will probably not be applicable for experiments of the type discussed here in the surface layer. Instead we can await the diffusion to proceed more like the fixed system type, but with reduced variance. To have the real fixed system type diffusion, we must also take into account the displacement of the puff-centres relative to the fixed coordinate system. The motion of the centres will to some extent be influenced by wave-numbers which are effective in the relative diffusion, but most of the motion is produced by lower wave numbers. Now a continuous emission of 30-seconds-puffs is equivalent to a continuous source, and then the variance of the particle distribution at a fixed distance from the source is equal to the sum of the variance of the particle distribution relative to the puff centre and the variance of the distribution of centres, or in obvious mathematical notation:

$$\sigma^2 = \sigma_r^2 + \sigma_c^2. \tag{1}$$

This relation is true independently of the distance from the source. At moderate distances σ_c^2 and σ_r^2 can be said broadly to represent the effect of the low wave number part of the spectrum and the high wave number part respectively.

To effectively sample σ_c^2 the spread of several puff-centres must be taken into account. Usually one experiment consists of 4–6 puffs: puff no. 2 being released when puff no. 1 is not longer to be seen and so on. One full experiment will take about one hour which time can thus be regarded as the sampling time of the experiment. This time will be enough to sample even the lowest wave numbers which play any role of importance in the vertical diffusion, at least in thermally stable and near neutral conditions, which for other reasons are those conditions for which the method described here is most likely to give good results. But 4–6 values are not enough to get reliable results for the variance. Because of this, we combine the results from several experiments which have been carried out at similar conditions.

Unlike the spectrum of the vertical motion, the spectrum of the horizontal motion is extremly wide—according to OBUKHOV (1962) the scale extends from about 1 cm to 2500 km. This means that a great part of the total spectrum of the horizontal motion is not sampled in one hour. The very low wave numbers which have thus been filtered out show up in the veering of the entire one hour plume from hour to hour. We can combine results from several different experiments by computing the variance relative to a central axis made common for the different experiments. In this way the effective sampling time is not increased by using results from several experiments (made at similar conditions). Several investigations of horizontal turbulence spectra have shown (see for instance PANOFSKY & DELAND, 1959) that there is a marked minimum or even gap round frequency 1 hour^{-1}. These investigations refer to Eulerian time spectra, but the "gap" seems to be so wide that we can say with confidence that diffusion experiments carried out over one hour will sample all the "micrometeorological" part of the spectrum and very little of the "synoptic" part. To investigate the influence on diffusion of the "synoptic" part deserves a special technique.

Evaluation of the diffusion relative to the moving puff centre

CRAMER, RECORD and VAUGHAN (1958) have carefully examined results from tracer experiments made at O'Neill and Round Hill with sampling times varying from 30 seconds to 10 minutes. They conclude that the distribution of matter across wind does not significantly deviate from the normal error law for any of the sampling times. If this result is extended to three dimensions, the equation for the distribution of matter in an instantaneously emitted puff is:

$$\chi = \frac{Q}{2\sqrt{2}\pi^{3/2}\sigma_x\sigma_y\sigma_z} \exp\left[-\left(\frac{x^2}{2\sigma_x^2}+\frac{y^2}{2\sigma_y^2}+\frac{z^2}{2\sigma_z^2}\right)\right] \tag{2}$$

where Q is total amount of matter in the puff and σ_x, σ_y, and σ_z are the standard deviations of matter in three perpendicular directions (x along the mean wind, z vertically, origin in puff centre) at a given time after release.

If we integrate equation (2) over all x, we have:

$$G(y, z) = \frac{Q}{2\pi\sigma_y \cdot \sigma_z} \exp\left[-\frac{y^2}{2\sigma_y^2}-\frac{z^2}{2\sigma_z^2}\right]. \tag{3}$$

Now look at a puff which has been emitted during 30 seconds. At a given instant after release of the puff as a whole the particles in the foremost part of it are more widely scattered than those which are closer to the source. Imagine all the particles projected by the lines of sight from the observing point (= the source) on a plane perpendicular to x and situated exactly at the midpoint of the puff. In the earlier stages the particle standard deviation grows linearly with x. This means that the particles projected in the way described will be distributed exactly in the way described by equation (3), with σ_y and σ_z being relevant to the midpoint of the puff and to the sampling time 30 seconds. When the puff is more remote the diffusion increases slower than proportional to x. This means that distributions with somewhat different standard deviations are superposed at the plain in the midpoint of the puff. The resulting distribution is not exactly Gaussian in this case, but the divergence can hardly be of any practical importance.

Suppose now that a contour representing constant integrated concentration, G_0 can be identified, following the puff continuously from the time of release (or at least from 30 seconds after the puff centre has left the source) to the time of disappearance. This contour will be an ellipse with continuously changing axes $a = a(t)$ and $b = b(t)$. The equations for a and b are (from eq. (3)):

$$G_0 = \frac{Q}{2\pi\sigma_y \cdot \sigma_z} \cdot \exp\left[-\frac{a^2}{2\sigma_y^2}\right] \tag{4 a}$$

$$G_0 = \frac{Q}{2\pi\sigma_y \cdot \sigma_z} \cdot \exp\left[-\frac{b^2}{2\sigma_z^2}\right] \tag{4 b}$$

G_0 and Q are constants, but σ_y and σ_z grow monotonically with t. This means that a and b grow from zero to a maximum and then decline to zero. We make use of this fact to determine σ_y and σ_z from measurements of a and b. We differentiate eqs. (4a) and (4b) logarithmically with respect to t, make use of the fact that, from eqs. (4a) and (4b)

$$\frac{a}{b} = \frac{\sigma_y}{\sigma_z} \tag{5}$$

and find, combining the equations, that for the point where $da/dt = 0$:

$$\frac{db}{d\sigma_z} \cdot \left(\frac{a^2}{\sigma_y^2} - 1\right) = \frac{a^3}{\sigma_y^3} - \frac{2a}{\sigma_y}. \tag{6}$$

If db/dt is zero simultaneously with da/dt, then because $db/d\sigma_z = db/dt \cdot dt/d\sigma_z$:

$$\sigma_{y0} = \frac{a_0}{\sqrt{2}} \tag{7}$$

where a_0 means the value that a attains in the point where $da/dt = 0$, and σ_{y0} is the value of σ_y at the same point. When now a and σ_y are known for one point, the constant G_0/Q can be determined from eq. (4a). It is then possible to determine σ_y and σ_z for all points where a and b are known with the aid of eqs. (4a) and (4b).

If db/dt is not zero at the same time as da/dt, we can proceed in the following way. Suppose σ_z locally to be of the form $\sigma_z = Bt^p$. Then $d\sigma_z/dt = p\sigma_z t^{-1}$ and

$$\frac{db}{d\sigma_z} = \frac{db}{dt} \cdot \frac{dt}{d\sigma_z} = \frac{db}{dt} \frac{t}{p \cdot \sigma_z}. \tag{8}$$

As a first approximation σ_z is not very far from $b/\sqrt{2}$ (cf. eq. (5) and (7)), and $p = 0.8$. From this and eq. (8):

$$\frac{db}{d\sigma_z} \simeq \frac{db}{dt} \cdot \frac{2t}{b}. \tag{8 b}$$

Because db/dt and b can be measured, $db/d\sigma_z$ is known by first approximation and σ_y can be obtained by solving eq. (6). The value thus obtained can be used in eq. (5) to give a better approximation of σ_z. This value can then be put into eq. (8) to produce a better value for $db/d\sigma_z$ and so on. After a few iterations a stable value for σ_y (and then also for σ_z) has been obtained. Then the constant G_0/Q can be obtained from eq. (4a) which as in the special case described first is the starting point for computing σ_y and σ_z for all t for which a and b are known.

The pre-requisite for the described method to be applicable is that we can safely identify the integrated concentration line, G_0. The exact meaning of ROBERTS' "opacity theory" (cf. p. 205) is that providing the background against which the puffs are viewed is uniformly illuminated during the whole experiment, then a certain threshold value of the integrated concentration is interpreted as the contour of the cloud. Taking this for true, a and b can be obtained by the following method, which has been used in the present investigation. The weakness of the assumptions will be discussed on page 209.

As already described (p. 205) the puffs are photographed from a point very close to the point of release (in practice the photo-point is often situated a few metres below the point of release, so that a small correction for parallax will be necessary as long as the puff is close to the source). The first exposure of the puff is in most cases taken 60 seconds after the mid-point

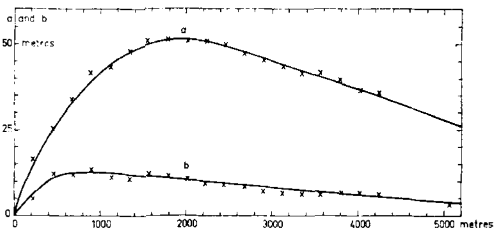

FIG. 1. Typical example showing the quantities a and b as measured from an experiment performed at the 87 m level in Studsvik. Cf. the text.—Moderate inversional conditions. Date and time of experiment: 9.9.1960 0511–0617.

of the puff has left the source. The subsequent exposures are taken with intervals 15 sec, 30 sec or 60 sec according to whether the diffusion is fast or slow. As 24 × 36 mm film with 36 exposures is used, an interval is chosen so that there will be either 18 or 36 exposures of one puff. For cases with fast diffusion an objective with focal length 50 mm is used. In most inversional cases an objective with focal length 135 mm or more is used.

The negatives are projected suitably magnified on to white paper. An operator fills in with a pencil what in his opinion is the contour of the puff. He also delineates the horizon and some characteristic feature in the background —the same feature in all the pictures of one experiment because this feature and the horizon provide the necessities for fixing the absolute system of reference needed for the computation

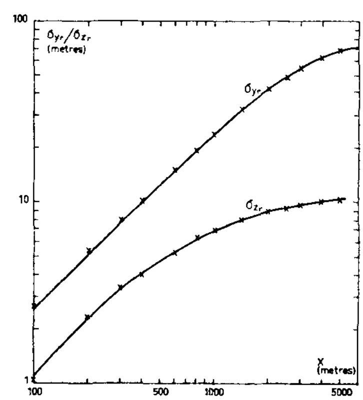

FIG. 2. Typical example showing the horizontal cross wind and vertical standard deviation of particles relative to the moving puff centre as computed from puff photographs. Same experiment as in Fig. 1.

of the spread of the puff centres that is for the determination of σ_{yc} and σ_{zc}.

To be able to compute a and b from the measurements of the vertical and horizontal dimensions of the oval that constitute the puff, it is necessary to know the distance from the camera to the puff when the exposure was taken. This is accomplished by postulating that the distance, x

$$x = \bar{u}t \tag{9}$$

where $\bar{u}$ is the mean wind speed at the point of release over the time the puff is discernible. This postulate will be discussed later.

For each distance means are taken of the values obtained for a and for b from the different puffs of the experiment in question. Fig. 1 shows a typical example of the results obtained for one certain experiment. The corresponding σ_y's and σ_z's, calculated with the aid of eqs. (4a) and (4b), are displayed on a log-scale against $\log x$ in Fig. 2.

Critical examination of the method

As described earlier, the total variance of the particle distribution in the fixed system at a certain distance from the source is the sum of the variance of particle distribution relative to the moving puff centre, σ_r^2 and the variance of the distribution of centres, σ_c^2 (eq. (1)). We will now examine the sources of error in the determination of σ_r and σ_c.

To begin with σ_c, this quantity is simply determined as

$$\sigma_c = \sqrt{\frac{\sum_{i=1}^{n} y_i^2}{n}} \tag{10}$$

where y_i is the departure of the ith puff centre from the mean value of y (taken to be zero). We will postpone the discussion of what uncertainty will arise as the result of too few puffs being used, that is of using a finite n in eq. (10). Apart from occasional errors, as those resulting from difficulties in finding the correct position of the centre of gravity in some cases, the main source of error is probably the use of the mean wind, $\bar{u}$ in the determination of the distance x between source and puff centre (see eq. (9)), and so in the computation of y_i. But the centres travel in approximately straight lines from the source over fairly long distances (of the order of a kilometre). This means that a centre which is really at the point $(x; y)$ is wrongly interpreted from the picture as being at $(kx; ky)$. But if the centre moves approximately in a straight line from the source, it will at another moment really be at $(kx; ky)$, so that approximately the correct trajectory in the $(x; y)$-plane is obtained in spite of the incorrect $\bar{u}$-value.

At greater distances from the source the particles move in widely different directions. A given error, $\Delta\bar{u}$ in the determination of the appropriate mean wind $\bar{u}$ in eq. (9), will then produce positive errors for some particles and negative for others. But the net effect of these errors will not be zero in the general case. The quantity $\overline{|y|}$ is proportional to σ_c, the factor of proportionality being $\sqrt{\pi/2}$ in the Gaussian case. But at great distances from the source σ_c and hence $\overline{|y|}$ is proportional to $\sqrt{x}$ (see p. 221). From a simple figure it is seen that the error in $\overline{|y|}$ is $(\overline{|y|}/2)\,(\Delta\bar{u}/\bar{u})$ and then the error in σ_c

$$\Delta\sigma_c = \frac{\sigma_c}{2}\frac{\Delta\bar{u}}{\bar{u}}.$$

At a typical wind speed of 5 m/sec the error $\Delta\bar{u}$ will probably seldom exceed 0.5 m/s so that normally the percentage error in σ_c will be less than about five percent. This conclusion is confirmed by the results from the investigations at the level 87 m in Studsvik. As is shown in detail in part IV the puffs released from the level 87 m in landward directions, have mean trajectories that very closely follow the topography in the vertical. The correlation between trajectory and relevant topography profiles could not have been so high if the error in the determination of the coordinates of the centres due to the error in $\bar{u}$ had been of importance, or especially if the measured wind value at the point of release had been significantly and systematically different from the trajectory mean in eq. (9).

We will now discuss the possible sources of error to the determination of σ_r, the standard deviation of the particles relative to the moving centre.

1. Departure from the assumed Gaussian distribution of matter within the puff. Systematic departures are not very likely to occur, but because there are turbulent wavelengths comparable to the size of the puff, these will introduce distortions of the puffs. This is very

pronounced in thermally unstable conditions, but becomes less important as stability increases. In inversion conditions the puffs are mostly very regular ovals (apart from the regular distortion introduced by wind direction shear, cf. next section). The small remaining irregularities are smoothed out by computing a and b as means from four to six puffs which constitute one experiment. This is at least true for inversional and near neutral conditions.

2. Reduced visibility, non-uniform back ground, considerable change of the illumination, or other conditions which invalidates the "opacity theory". Experiments which are clearly subject to such conditions are rejected, and among the accepted experiments remaining interference of effects of this type will be sporadic and of little importance.

3. The possible invalidity of the "opacity theory" as such. This problem can suitably be expressed as two questions. Firstly, will a line of constant integrated concentration be reproduced as a line of constant blackness on the film (provided the illumination does not change during the experiment)? Secondly, is what the operator takes as the "boundaries" of the puff on the different pictures identical with a line of constant blackness?

The first question will with confidence be answered: yes, at least in the outer parts of the puff (the dense parts of the puff may be self-screening). The statement is very likely to be true not only for black clouds against a brighter background, as in ROBERTS' original treatment, but also for bright clouds against a darker background. This can be shown in an elementary but somewhat lengthy way with the aid of well known optics (see HÖGSTRÖM, 1959).

The other question can not be answered so promptly. Most authors who have used smoke puffs for diffusion studies assume the answer to be yes. FRENKIEL & KATZ (1956) do so too, but remark that "studies of contour perception seem to show that the value of the second derivative of the luminous intensity is particularly significant in the contour formation". At least near the source, where the distribution curve is very peaked, the results will differ little if the puff contour is taken as a line of constant integrated concentration or as a line of constant second derivative in integrated concentration. A good illustration to the applicability of the procedure accepted here is given by GIFFORD (1957) who successfully verified the existence of a $t^{\frac{3}{2}}$-region in relative diffusion of instantaneously generated clouds with the aid of the results from the smoke puff experiments of KELLOGG and of FRENKIEL & KATZ.

At greater distances from the source there may be introduced a systematic error in the determination of σ_r, if the remark of FRENKIEL & KATZ is correct. But this error, if existing, will probably introduce rather small errors in the determination of the total standard deviation, σ, because σ_c is then often greater than σ_r (cf. eq. (1)). The results to be presented in this paper strongly justify the adopted method.

2. Presentation of the experimental results. Description of the stability dependence of the particle standard deviation

The method described in sec. 1 has been used in a rather extensive investigation at two places in Sweden: Ågesta, just outside Stockholm, and Studsvik, situated about 100 km SSW of Stockholm. The topography of the two places is rather similar in character: there are stony hills covered with mostly coniferous trees, and in between rather small areas of arable and pasture land and also minor lakes. The height differences between the hills and the valleys are mostly a few decametres and seldom more than 50 metres. There is however one important topographical difference between the places: Ågesta is situated well inside an appreciable area of the described character while Studsvik, located just at the shore of the Baltic, can be said to be situated at the border of such an area. Although there is a shielding chain of islands outside Studsvik, the influence of the topographical discontinuity on the diffusion pattern is remarkable, as will be seen from the analysis.

The experiments were carried out during the years 1960–1963. As the main interest lay in the inversional conditions, most experiments were performed near sunrise, or just as early as illumination conditions allowed. Here is a short summary of the experiments:

1. Studsvik, release from the top of the 87 m high chimney of the reactor R2, situated 200 metres from the shore, 18 m above sea level; the puffs photographed from a platform at the chimney, 15 m below the top (a correction for

parallax being applied in the evaluation); number of experiments 72, which means nearly 300 puffs in all.

2. Studsvik, release from the level 24 metres above ground on the meteorological mast, situated 500 metres northwest of the R2 chimney at a small hill, 35 metres above sea level; the puffs photographed from the proper point of release; number of experiments 18, including 64 separate puffs.

3. Ågesta, release from a tube 50 metres high, erected at the hill in which the Ågesta reactor is accommodated; the puffs photographed from a 30 m high mast in close connection to the smoke tube; number of experiments 21, including 70 puffs.

As mentioned above, there are pronounced local effects to be noticed in the Studsvik material which is not be seen in the material from Ågesta. It would then seem natural to analyse the last mentioned, more "ideal" material, first. But on the other hand, the experiments from the 87 m level in Studsvik are so much more numerous than those from the other levels that it seems most convenient to analyse the material from this level first.

a. Studsvik, 87 m level

The diffusion relative to the moving centre

Fig. 2 shows (on a logarithmical scale) σ_{y_r} and σ_{z_r} for one single experiment. The sample is very typical of most experiments: the puffs could be followed a few kilometres (in this case five kilometres), σ_y is greater than σ_z, both σ_y and σ_z grow linearly with x to begin with, σ_y then gradually approaches const. $\sqrt{x}$ while σ_z rather soon attains a state of "slower than Fickian diffusion", that is $\sigma_z = Cx^n$ with n less than 0.5. In other experiments one can see how σ_z approaches the asymptotic state const. $\sqrt{x}$ a little farther away from the source. In some experiments the peculiar "knee" in the ($\log \sigma_z$; $\log x$)-curve is not at all to be seen. It is thought that the knee is mainly a sampling effect caused by the puff being bounded in extension.

When comparing the results from different experiments one is immediately struck by the very pronounced effect of thermal stratification on both σ_{y_r} and σ_{z_r}. To find the most convenient stability parameter the quantity ${}^{10}\log(\sigma_{y_r}\cdot\sigma_{z_r})$ for $x = 2000$ m is displayed against the following combinations:

$$ {}^{10}\log\frac{\partial\theta}{\partial z};\ {}^{10}\log\left[\frac{\partial\theta}{\partial z}\Big/\left(\frac{\partial\bar{u}}{\partial z}\right)^2\right];\ {}^{10}\log\left[\frac{\partial\theta}{\partial z}\Big/\bar{u}_{72}^2\right]; $$

$$ {}^{10}\log\left[\frac{\partial\theta}{\partial z}\Big/\bar{u}_{122}^2\right] \quad\text{and}\quad {}^{10}\log\left[\frac{\partial\theta}{\partial z}\Big/u_f^2\right] $$

where $\partial\theta/\partial z$ = local vertical gradient of potential temperature, derived from measurements of the temperature at 30 m and 122 m level in the meteorological mast.

$\partial\bar{u}/\partial z$ = local vertical wind gradient, derived from measurements of the mean wind at 36 m, 72 m and 122 m on the mast.

$\bar{u}_{72}$ = mean wind at 72 m level on the mast.

$\bar{u}_{122}$ = mean wind at 122 m level on the mast.

u_f = "the free wind", that is the wind just above the friction layer. u_f was obtained in the following way. For routine purpose an interpolation series of hourly u_f-values was constructed from the mean wind in the layer round 500 m taken from the regular rawindsonde data for 00z and 12z for Bromma (situated about 100 km NNE of Studsvik) during all 1960, 1961 and most of 1962. The values used in this investigation was taken directly from this interpolation series.

In the diagrams thus constructed curves of best fit were drawn by eye. Then the correlation of the points to the curves was computed. The correlation showed to be appreciable for all the parameters used. ${}^{10}\log \partial\theta/\partial z$ and

$$ {}^{10}\log\left[\frac{\partial\theta}{\partial z}\Big/\left(\frac{\partial\bar{u}}{\partial z}\right)^2\right] $$

have the lowest values, round 0.85. The best correlation, 0.95 was obtained with $\lambda = {}^{10}\log[(\partial\theta/\partial z)/u_f^2]$ (see Fig. 3). This is especially remarkable when taking into account the great uncertainty in the determination of u_f. In part II there is given strong theoretical evidence for the use of the combination $(\partial\theta/\partial z)/u_f^2$ as a local stability parameter. Thus, we will use this parameter exclusively in the following treatment.

In Fig. 4 σ_{z_r}, that is the vertical standard deviation of the particles within a puff relative to its moving centre, for $x = 1000$ m is displayed on a logarithmic scale against

$$ {}^{10}\log\left[10^5\frac{\partial\theta}{\partial z}\Big/u_f^2\right]. $$

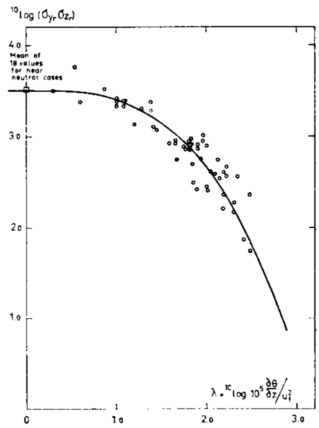

FIG. 3. Measurements of $(\sigma_{y_r}\sigma_{z_r})$ for $x = 2000$ m at the 87 m level in Studsvik displayed against the stability parameter $\lambda = {}^{10}\log[10^5(\partial\theta/\partial z)/u_f^2]$. The curve is drawn by eye to give best fit. Correlation $= 0.95$.

The curve drawn is

$$\sigma_{z_r} = \frac{27}{1 + 2.2 \cdot 10^{-2} s} \tag{11}$$

where

$$s = \left(\frac{\partial\theta}{\partial z}\bigg/ u_f^2\right) \cdot 10^5. \tag{12}$$

The analytic form (11) is remarkable as it is identical with that predicted in part II for the total standard deviation, σ_z (but with other

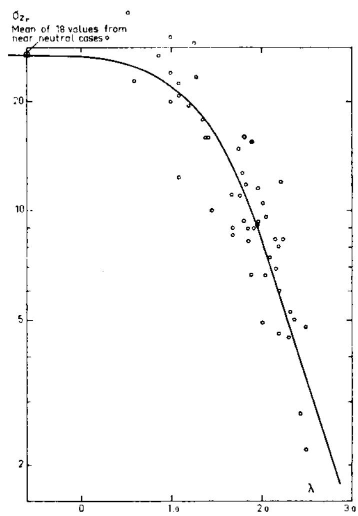

FIG. 4. Measurements of σ_{z_r} for $x = 1000$ m at the 87 m level in Studsvik displayed against the stability parameter $\lambda = {}^{10}\log[10^5(\partial\theta/\partial z)/u_f^2] = {}^{10}\log s$. The curve drawn is $\sigma_{z_r} = 27/(1 + 2.2 \cdot 10^{-2} \cdot s)$.

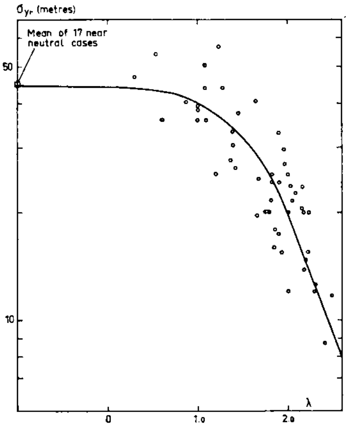

FIG. 5. Measurements of σ_{y_r} at $x = 1000$ m for the 87 m level in Studsvik displayed against $\lambda = {}^{10}\log[10^5(\partial\theta/\partial z)/u_f^2]$.

constants). Diagrams like Fig. 4 have also been constructed for several other distances up to $x = 4000$ m. These all show the same high correlation (about 0.95) to the curve

$$\sigma_{z_r}(x, s) = \frac{\sigma_{z_r}(x, 0)}{1 + 2.2 \cdot 10^{-2} s} \tag{11 b}$$

where $\sigma_{z_r}(x, 0)$ is the value of σ_{z_r} at the distance x for neutral conditions.

In Fig. 5 σ_{y_r} for $x = 1000$ m is shown in exactly the same representation as σ_{z_r} in Fig. 4. The figures are similar in all respects. σ_{y_r} shows the same high correlation to s at other distances.

The dispersion of the centres of the puffs

Horizontal diffusion. As discussed in sec. 1 (p. 207) it is necessary to put together in groups several experiments carried out in similar conditions. The stability parameter, s, was used as a basis of division. The experiments were assigned to one of eight classes as comes out of Table 1, column 1.

The quantity y_i^2 where y_i is the departure of the ith puff centre from the mean value of y, was computed for each of the c. 25 puffs of every group for the distances shown in the table. Then

$$\sigma_{y_1} = \sqrt{\frac{\sum y_i^2}{n}} \tag{13}$$

was computed. The quantity s has a chi-square

TABLE 1. *Determination of* $\sigma_{y_1} = \sqrt{\sum y_1^2/n}$ *for the centres of the puffs. The expected uncertainty computed with eq.* (14). *The values given in the table are not corrected for wind direction shear.*

	250 m		500 m		1000 m		1500 m[a]		2000 m[a]		2500 m[a]		3000 m[a]		4000 m[a]		5000 m[a]	
	n	$\frac{\sqrt{\Sigma y^2}}{n}$	n	$\frac{\sqrt{\Sigma y^2}}{n}$	n	$\frac{\sqrt{\Sigma y^2}}{n}$	n	$\frac{\sqrt{\Sigma y^2}}{n}$	n	$\frac{\sqrt{\Sigma y^2}}{n}$	n	$\frac{\sqrt{\Sigma y^2}}{n}$	n	$\frac{\sqrt{\Sigma y^2}}{n}$	n	$\frac{\sqrt{\Sigma y^2}}{n}$	n	$\frac{\sqrt{\Sigma y^2}}{n}$
neutral	35	17 ± 2	37	33 ± 5	37	74 ± 10	29	82 ± 15	23	114 ± 16	16	137 ± 20	—		—		—	
$\lambda = 0.30$–1.0	24	18 ± 2	29	44 ± 5	29	85 ± 10	25	110 ± 15										
$\lambda = 1.08$–1.36	20	13 ± 2	20	19 ± 5	19	38 ± 10			21	105 ± 16			8	217 ± 40	—		—	
							22	57 ± 15			18	114 ± 20						
$\lambda = 1.38$–1.65	22	16 ± 2	22	32 ± 5	22	59 ± 10												
							24	75 ± 15										
$\lambda = 1.67$–1.84	24	15 ± 2	24	29 ± 5	24	50 ± 10			24	94 ± 16	19	123 ± 20	13	164 ± 40	—		—	
							18	114 ± 13										
$\lambda = 1.88$–2.00	28	17 ± 2	28	32 ± 5	28	58 ± 10			21	130 ± 16								
							26	92 ± 15			18	155 ± 20	12	201 ± 40	14	290 ± 50	7	399 ± 10
$\lambda = 2.03$–2.18	20	16 ± 2	20	32 ± 5	20	71 ± 10			17	141 ± 16								
$\lambda = 2.19$–2.48	21	17 ± 2	21	32 ± 5	19	45 ± 10	22	85 ± 15	14	92 ± 15	17	141 ± 20	13	187 ± 40				

[a] The stability grouping given in column 1 is quite correct only for 250 m, 500 m and 1000 m; for the other distances the figures have been displaced vertically in the table to indicate the true λ-limits. n is number of puffs in the group in question.

distribution. The uncertainty of σ_{y_1} has been derived as

$$\varepsilon = \pm \frac{\sigma_{y_1}}{\sqrt{2n}} \tag{14}$$

and inserted in Table 1.

As is clearly seen from Tab. 1 *there is no significant dependence of* σ_{y_1} *on stability.* Mean values have been computed for each distance, and the values have been plotted as rings in Fig. 6. Estimated errors computed with the aid of eq. (14) are indicated as vertical lines. The result reveals, that there are other effects in action than pure turbulent diffusion because, for the fixed type diffusion under consideration,

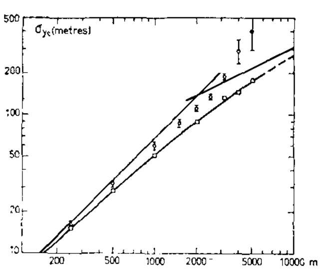

FIG. 6. Horizontal dispersion of the puff centres. The rings indicate the values derived directly from eq. (13). The squares are the values obtained when the effect of the wind direction shear is taken into account. 87 m level in Studsvik.

there is no reason to expect accelerated diffusion. We will now take into consideration the effect of the wind direction shear, studied in part V of this paper.

The parameter we want to derive is (σ_{y_1} being as above the observed standard deviation of the puff centres):

$$\sigma_{y_c} = \sqrt{\sigma_{y_1}^2 - \overline{y_s^2}} \tag{1 a}$$

where $\overline{y_s^2}$ is the horizontal variance introduced by the wind direction shear. It is to be computed from eq. (114) (p. 248):

$$\overline{y_s^2} = \frac{\psi^2 \sigma_z^2(x) x^2}{2(\alpha + 1)}. \tag{114}$$

In this equation ψ is the turning of the wind in radians per metre. α is a constant (cf. p. 248) which can be assigned the value 0.65. Statistics of ψ has been gathered over seven months in Studsvik and in Ågesta. The values of ψ measured on the meteorological mast in Studsvik, 450 metres from the line of topographical discontinuity (= the shore), cannot be expected to be representative for very large areas. It is very reasonable to believe that ψ soon after the passage of the shore attains about the same values as in Ågesta. The mean measured direction shear for the layer 36–122 metres is 12°, viz. $\psi = 2.4 \cdot 10^{-3} m^{-1}$. The corresponding σ_z's for the different distances are taken from Table 2, p. 215. In inversion conditions ψ is considerably greater than in near neutral conditions, but σ_z is correspondingly smaller, so that, to the first approximation, $\overline{y_s^2}$ is independent of stability. This leads to the very interesting conclusion, that *the horizontal turbulent diffusion that affects the centres of the puffs is independent of stability* (that is σ_{y_c} is independent of stability) *in striking contrast to what is the case of the diffusion relative to the centres* (that is σ_{y_r}). This can be interpreted qualitatively in the following way.

The influence of stability is primarily on the vertical component of turbulence only. But the fluctuating pressure forces strive to equalize the energy of the different eddy components (see BATCHELOR, 1959). This is done quite effectively for the higher wave numbers, and complete isotropy results in the Kolmogoroff region. But the equalizing effect strongly declines with decreasing wave numbers. This is felt already in the anisotropy observed for σ_{y_r}. For those wave numbers effective in the dispersion of the centres no appreciable effect is present at all.

We now return to the quantitative treatment, and put in the relevant parameters in eq. (114) and eq. (1a). The computed σ_{y_c}'s are plotted as squares in Fig. 6. The result is just what one would expect from the theory (cf. BATCHELOR, 1949): $\sigma_{y_c} \sim x$ for small x and $\sim \sqrt{x}$ for great x. It is sometimes argued (see PASQUILL, 1962*b*) that the asymptotic state $\sigma \sim \sqrt{x}$ should never be reached in the atmosphere for horizontal diffusion, because of the enormous range of the horizontal eddy spectrum. But when taking into account the experimental fact (cf. p. 207) that this spectrum has a very pronounced minimum for periods of the order of an hour, it seems very natural that this state is really attained for sampling times of about one hour.

With the aid of eq. (1) the total σ_y for 1 hour sampling can be computed, when knowing σ_{y_r} and σ_{y_c}:

$$\sigma_y^2 = \sigma_{y_r}^2 + \sigma_{y_c}^2. \tag{1 b}$$

Because σ_{y_r} varies with stability there will also be a slight variation in σ_y with stability. In Fig. 7 the curves for neutral conditions,

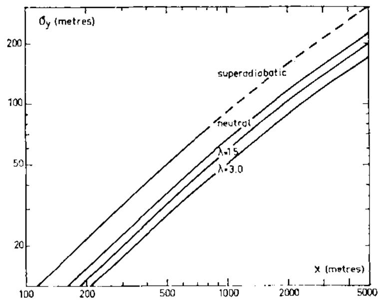

FIG. 7. Total horizontal dispersion parameter, σ_y for 1 hour sampling time. 87 m level in Studsvik.

for $\lambda = {}^{10}\log s = 1.5$ (cf. eq. (12) p. 213) and for $\lambda > 3.0$ has been drawn together with a very uncertain curve for slightly superadiabatic conditions (based only on 15 puffs).

Vertical diffusion. The horizontal diffusion showed no significant variation with wind direction nor did the vertical diffusion relative to the centres of the puffs. The vertical diffusion of the puff centres however, varies markedly with wind direction at Studsvik. The details of this behaviour of the puffs are treated at length in part IV of this paper. Suffice it here to say, that conditions are quite different when the wind blows towards the land and from the land, and further that in the land-ward case the mean trajectories of the puffs are streamlines at constant height = 87 m above the underlying ground. The land-ward case will be exclusively treated below.

Synthesis of the σ_z-results for the land-ward case for the 87 m level in Studsvik

From the curves for σ_{z_r}, that is for the vertical diffusion relative to the moving centre (Fig. 4 and corresponding curves for other distances) and the curves for σ_{z_c} (Fig. 8) values have been extracted for several distances—see Tab. 2, where σ_{z_r} has been inserted in the first line for every distance and σ_{z_c} in the second line. The total standard deviation, σ_z has been computed with the aid of eq. (1) and the result has been inserted in the third line for every distance. The σ_z-values have been plotted against x in a log–log-representation (Fig. 9) and curves have been drawn through the points.

We will now try to find an analytical expression for σ_z as a function of x and of s. The following simple analytical form will be tested:

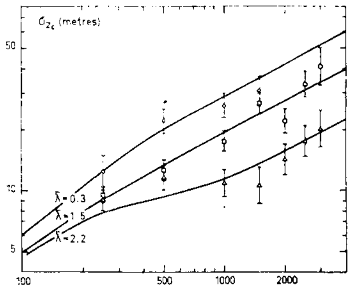

FIG. 8. 87 m level in Studsvik. σ_{z_c} for the landward cases (wind from 350°, 360°, 010° ... 170°, 180°). Each point in the diagram has been computed from the formula $\sigma_{z_c} = \sqrt{\sum z_i^2/n}$ where n is the number of puffs (usually about 20).

Legend △ $\lambda \geqslant 2.0$, □ $1.0 \leqslant \lambda < 2.0$, ○ $\lambda < 1.0$.

$$\sigma_z = \sigma_{z_a}(x)\,\frac{1}{1+b(x)}\left[\frac{1}{1+as} + b(x)\right] \tag{15}$$

where $\sigma_{z_a}(x)$ is the value for σ_z at x for neutral stability.

Table 2 gives measured σ_z for three different stabilities for every distance. We form with the aid of eq. (15) the following quantity to be determined for each distance

$$k = \frac{\sigma_{z_1} - \sigma_{z_2}}{\sigma_{z_1} - \sigma_{z_3}} = \frac{(s_2 - s_1)(1 + as_3)}{(s_3 - s_1)(1 + as_2)}. \tag{16}$$

The λ-values in Tab. 2 correspond to the following s-values (for the definition of s, see eq. (12)):

$$s_1 = 2.0$$
$$s_2 = 31.5$$
$$s_3 = 178.$$

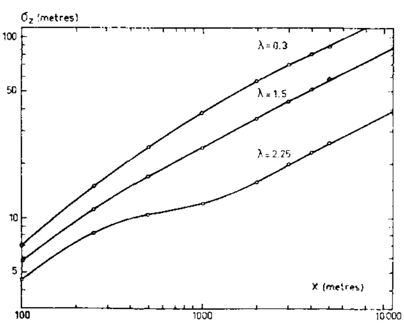

FIG. 9. Studsvik 87 m level. Total vertical standard deviation, σ_z (sampling time abt. 1 hour) for landward winds. See also table 2 and the text.

TABLE 2. *Studsvik 87 m level (landward cases). Vertical standard deviation (metres). The values in the first line for each of the distances are σ_{z_r}, taken from diagrams like Fig. 4. The values in the second line are σ_{z_c}, taken from the curves drawn in Fig. 8. The values in the third line are $\sigma_z = \sqrt{\sigma_{z_r}^2 + \sigma_{z_c}^2}$*

$x \diagdown \lambda$	0.3	1.5	2.25
	3.3	2.6	0.9
100	6.2	5.2	4.5
	7.0	5.8	4.6
	8.0	6.0	2.0
250	12.7	9.4	8.0
	15.0	11.2	8.2
	14.5	11.0	3.2
500	20.0	12.8	10.0
	24.7	16.9	10.5
	25.0	17.1	4.2
1000	29.0	17.8	11.2
	38.3	24.7	12.0
	39.5	25.0	6.8
2000	42.0	25.0	14.4
	57.6	35.4	15.9
	47.5	32.0	8.1
3000	51.0	30.0	18.1
	69.5	44.0	19.8
	54.5	37.5	9.5
4000	59.5	35.2	21.0
	80.5	51.0	23.0
	58.0	43.0	10.7
5000	67.0	40.0	23.7
	88.0	59.0	26.0

Table 2 and eq. (16) give:

$x(m)$	k
100	0.50
250	0.56
500	0.55
1000	0.52
2000	0.53
3000	0.52
4000	0.52

Average value of $k = 0.527$

Thus the quantity k does not vary significantly with x. Then the quantity a of eq. (15) is also a constant. Putting $k = 0.527$, eq. (16) gives

$$a = 2.7 \cdot 10^{-2}.$$

With the aid of eq. (15) and the σ_z-values given in Tab. 2, σ_{z_a} and b can be computed for each of the distances listed in Tab. 2. The following is obtained:

x	σ_{z_a}	b
100	7.18	1.32
250	15.4	0.75
500	25.5	0.40
1000	40.1	0.183
2000	60.2	0.120
3000	72.4	0.146
4000	84.0	0.146

The values thus obtained for $b(x)$ suggest the form:

$$b = b_1 e^{-\alpha x} + b_\infty. \tag{17}$$

From a plot of ${}^{10}\log(b_c - b_\infty)$, b_c being the b-values of the table above, against ${}^{10}\log x$ for some different values of b_∞ it is seen that the form (17) is fit excellently:

$$b = 1.8\, e^{-4.3\cdot 10^{-3}x} + 0.15. \tag{17 a}$$

The analytical form of $\sigma_{z_a}(x)$, that is of the vertical standard deviation at neutral stability, will be discussed in detail in part IV of this paper.

b. Studsvik, 24 m level

As mentioned earlier (p. 212) 18 experiments were performed from the 24 m level in Studsvik. The σ_{z_r}'s and σ_{y_r}'s, that is the standard deviation relative to the moving puff centre, show the same high correlation to the stability-parameter s as for the 87 m level. The curves for the 24 m-level are also of the $1/(1+\alpha s)$ form (cf. p. 213 and Fig. 4 and 5).

Ten of the eighteen experiments were "landward cases". The mean trajectories of these puffs showed the same pronounced tendency to be streamlines parallel to the underlying topography, as did the land-ward puffs for the higher level. The 10 land-ward experiments consisted of 38 puffs in all. This number is too small for giving significant results for $\sigma_{z_c}(s)$, that is for the standard deviation of the puff centres, if the puffs be divided among several different stability groups. As there was only one experiment, with two puffs, carried out in near neutral conditions, this experiment was rejected and the other taken all together. The mean λ (for the definition of λ, see eq. (12)) for these remaining nine experiments was 1.95. The computed σ_{z_c}'s for this group are plotted in Fig. 10, with estimated errors (cf.eq. (14), p. 214). As seen from Fig. 10, the 24 m puffs could not be followed for such long distances as the 87 m puffs could; most 24 m puffs disappeared at about 1 km from the source.

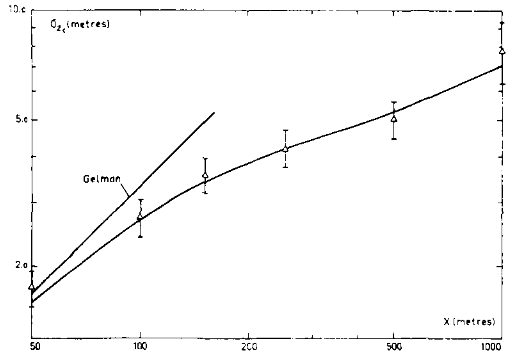

Fig. 10. Studsvik, 24 m level. σ_{z_c} computed from the trajectories of 36 puffs released at stable stratification. Average λ for the experiments is 1.95. The straight line labelled "Gelman" is the asymptotic state $\lim_{x\to 0}\sigma_z/x = \sqrt{\overline{\psi^2}}$ and is obtained from turbulence measurements; ψ is the azimuth of the particle trajectories when they leave the source.

Close to the source the particles move in straight lines. This means that

$$\lim_{x\to 0}\frac{\sigma_z}{x} = \sqrt{\overline{\psi^2}} \tag{18}$$

where ψ is the angle that the trajectories make with the x-axis, provided the field of turbulence is sufficiently homogeneous. Then an angle measuring device can be used to study the behaviour of σ_z for small x, and then used as a check to the entirely independent puff measurements. For this purpose a very light-weight bivane, type Gelman was installed in Studsvik. According to the manufacturers "at wind speeds of 6 miles/hour or above, all wind direction fluctuations up to ½ CPS are accurately recorded".

An electronic device of the type described by Jones & Pasquill (1959) was constructed to simplify the evaluation of the $\sqrt{\overline{\psi^2}} = \sigma_z/x$-statistics. Two sampling times were used: $\tau = 30$ sec and $\tau = 1000$ sec, which were thought broadly to correspond to the sampling times for σ_{z_r} and σ_z respectively. The electronic device was calibrated by running the original

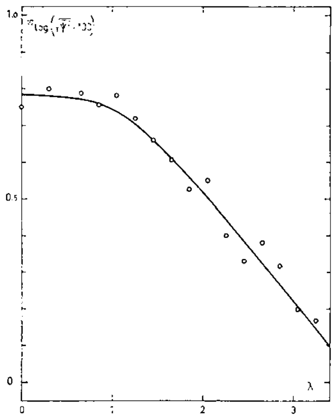

FIG. 11. Studsvik 24 m level. ${}^{10}\log(\sqrt{\overline{\psi^2}}\cdot 100)$ obtained from turbulence measurements. Sampling time 30 seconds. ψ is the azimuth of the particle trajectories when they leave the source.

signal, ψ parallel to the filtered signal for some time and then computing $\sqrt{\overline{\psi^2}}$ directly.

For the shorter sampling time ($\tau = 30$ sec) hourly averages for a two month material were divided into stability groups (c. 30 values in each group) and means were computed. The result is displayed in Fig. 11. A best fit curve is easily drawn. This curve appeared to agree almost exactly with the best fit curve of a logarithmic representation of the quantity ${}^{10}\log\,(100\cdot\sigma_{z_r}/x)$ against ${}^{10}\log x$; σ_{z_r} being taken from the puff measurements.

The same procedure as that described above

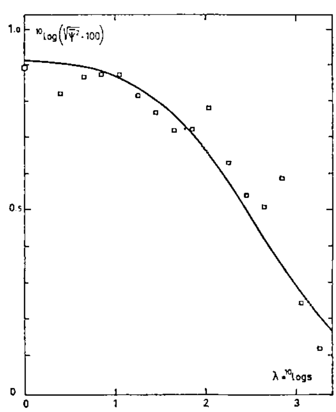

FIG. 12. Studsvik 24 m level. ${}^{10}\log(\sqrt{\overline{\psi^2}}\cdot 100)$ obtained from turbulence measurements. Sampling time 10^3 seconds. ψ is the azimuth of the particle trajectories when they leave the source.

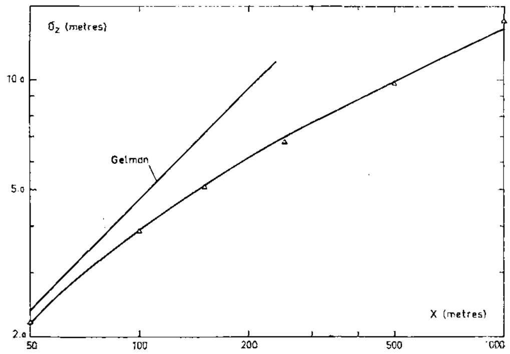

FIG. 13. Studsvik. 24 m level. σ_z for $\lambda = 1.95$. The line labelled "Gelman" is the asymptotic state $\lim_{x\to 0}(\sigma_z/x) = \sqrt{\overline{\psi^2}}$ and is obtained from turbulence measurements. ψ is the azimuth of the particle trajectories when they leave the source.

for the turbulence measurements for $\tau = 30$ sec was also performed for $\tau = 10^3$ sec. The computed values have been plotted in the same kind of diagram as the values for the shorter sampling time, see Fig. 12. The scatter of the points is somewhat greater than in Fig. 11, but it is still easy to draw a curve of best fit by hand.

From Fig. 11 and 12 the quantity

$$\sqrt{\overline{\psi_c^2}} = \sqrt{\overline{\psi^2_{\tau=10^3}} - \overline{\psi^2_{\tau=30}}} \tag{19}$$

can be derived. If the field of turbulence is sufficiently homogeneous the quantity (19) should equal σ_{z_c}/x for small x. From the curves

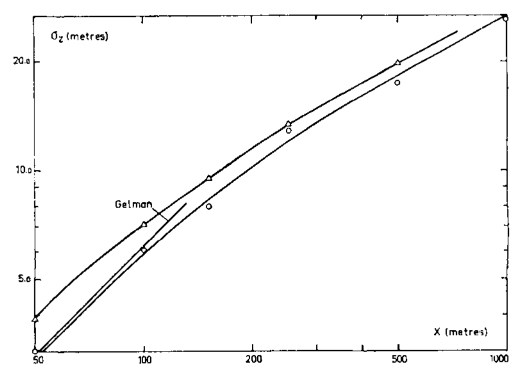

FIG. 14. Studsvik. 24 m level, neutral stability. The rings represent σ_{z_r} as taken from plots of ${}^{10}\log\,\sigma_{z_r}$ against λ for different x. The line labelled "Gelman", cf. Fig. 13. The triangles represent total σ_{z_a}. The points are derived with the aid of eqs. (15), (20) and (21) from σ_z-values for $\lambda = 1.95$ taken from Fig. 13.

in Fig. 11 and 12 values are taken for $\lambda = 1.95$ and inserted in eq. (19). The result is then displayed as a line in Fig. 10.

$$^{10}\log \sigma_{z_c} = {}^{10}\log \left(\sqrt{\overline{\psi_c^2}} \cdot x\right).$$

This line is seen to be a most probable asymptote to the curve ($^{10}\log \sigma_{z_c}$; $^{10}\log x$).

σ_z has been derived for $\lambda = 1.95$ from the puff measurements and the formula $\sigma_z = \sqrt{\sigma_{z_r}^2 + \sigma_{z_c}^2}$, and values taken from best fit lines of σ_{z_r} for different distances and from Fig. 10 for σ_{z_c}. The result is plotted in Fig. 13. The corresponding "Gelman-asymptote" from Fig. 12 is drawn and is seen to fit excellently.

It is now supposed that the "Gelman-result" $\sqrt{\overline{\psi^2}}$ is equal to σ_z/x not only for $\lambda = 1.95$ but for the whole range of λ. The points in Fig. 12 suggest eq. (35) to be applicable also for the level 24 m. Several combinations of the parameters a and b_0 (where b_0 is the value of b at small x) are possible. The curve drawn in Fig. 13 is

$$\frac{\sigma_z(s)}{\sigma_{z_a}} = \frac{\dfrac{1}{1 + 1.17 \cdot 10^{-2} \cdot s} + 0.2}{1.2}. \qquad (20)$$

It is not possible to determine the function $b = b(x)$ with great precision from the evidence presented. The value of b at great x, b_∞ can, however, not be very much different from zero. Supposing for instance $b_\infty = b_0 = 0.2$ gives a σ_z at $x = 1000$ m, which is less than the measured σ_{z_r}-value at that distance. It seems reasonable to propose the following form (cf. eq. (17a) p. 217):

$$b = 0.2\, e^{-4.3 \cdot 10^{-3} x}. \qquad (21)$$

Eqs. (15), (20) and (21) then make it possible to derive values for $\sigma_{z_a}(x)$, when $\sigma_z(x, s_1)$ is known ($s_1 = 89$, corresponding to $\lambda = 1.95$); The result is plotted as triangles in Fig. 14, but the discussion of the function $\sigma_{z_a} = \sigma_{z_a}(x)$ is postponed (see p. 243).

The horizontal diffusion for the level 24 m has also been examined. The σ_{y_r}-values exhibit the same strong stability dependence as does σ_{y_r} for the level 87 m. When the y^2-values for the 38 puffs are examined there is no significant variation with stability to be noticed (such a variation is very clear for z^2, but the estimated errors for the values are so great, when the puffs

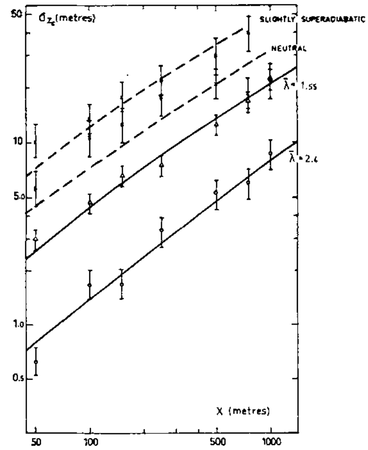

Fig. 15. Ågesta. 50 m level. σ_{z_c} computed from the trajectories of the puff centres. Legend: s: slightly superadiabatic (10 puffs), x: near neutral (14 puffs), $\triangle$: $\bar{\lambda} = 1.55$ (33 puffs), $\circ$: $\bar{\lambda} = 2.40$ (13 puffs). Concerning the curves drawn for the neutral and the superadiabatic cases, see the text.

are combined in small groups, that there is little chance to find a relation like eq. (20) this way). To sum up, the horizontal diffusion for the 24 m-level behaves qualitatively speaking exactly in the same way as it does for the 87 m-level.

c. Ågesta, 50 m-level

The σ_{z_r}-values for the 21 experiments in Ågesta show the same high correlation to a curve $1/(1 + \alpha s)$ as do the corresponding points for the two Studsvik levels.

The mean trajectories at Ågesta show no significant tendency to follow the topography. They are simply horizontal lines. It is possible that this is not true for a special case, namely for the combination of near neutral stability and westerly to north-westerly winds, that is for winds perpendicular to a rather marked valley straight west of the release point. As a matter of fact all 4 neutral case experiments from 50 m were carried out with winds from that sector. When computing σ_{z_c} for these four experiments, that is the standard deviation of the puff centres relative to a supposed horizontal mean trajectory, this means too great values up to a few hundred metres from the source. This is clearly seen from Fig. 15. The crosses are the points computed from the 14 neutral

TABLE 3. *Ågesta, 50 m level. Vertical standard deviation. The first line for each distance gives σ_{z_r} which are taken from best fit curves in ($^{10}\log \sigma_{z_r}$; $^{10}\log s$)-representations. The second line for each distance gives σ_{z_c} taken from the curves of Fig. 15. The third line gives the total standard deviation, σ_z.*

$x \diagdown \lambda$	$-\infty$	1.55	2.40
	2.3	1.2	0.25
50	4.5	2.5	0.79
	5.0	2.0	0.83
	4.6	2.4	0.63
100	7.0	4.6	1.35
	8.3	5.2	1.49
	7.4	3.6	0.71
150	9.6	6.0	1.88
	12.2	7.0	2.00
	11.7	5.8	1.50
250	13.5	8.6	2.87
	17.8	10.4	3.24
	23.7	10.8	2.00
500	21.0	13.5	5.00
	31.6	17.3	5.40
	27.5	12.3	2.70
750	27.0	17.2	5.90
	38.5	21.0	6.48
	33.5	14.4	3.35
1000	32.0	20.4	7.1
	46.2	25.0	7.9
		24.0	4.5
2000			9.8
			11.0
			5.9
3000			11.2
			13.0
			6.4
4000			13.2
			14.7

puffs. The s's are points derived from 10 puffs released in slightly unstable conditions. The triangles represent a group of 33 puffs with mean $\lambda = 1.55$. The circles represent a group of 13 puffs, released in very stable conditions, mean $\lambda = 2.40$. There is not much choice when drawing the lines of best fit for the last mentioned two groups. The line for neutral stability is drawn very tentatively.

As done for the two levels in Studsvik, values for σ_{z_r} are drawn from curves of best fit (($^{10}\log \sigma_{z_r}$; λ)-representation; cf. Fig. 4). The values for σ_{z_c} are taken from the curves in Fig. 15. Then

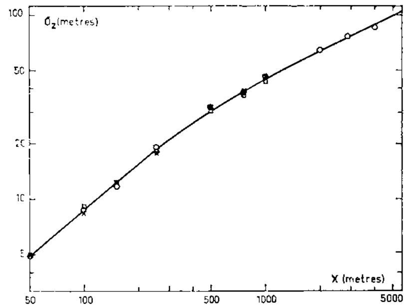

FIG. 16. Ågesta, 50 m level, "Normalized" σ_z-values. Crosses are the values for neutral stability taken from Tab. 3. Squares are the values for $\lambda = 1.55$ multiplied by the constant factor 1.755. Circles are the values for $\lambda = 2.4$ multiplied by 5.85.

σ_z is computed from the formula $\sigma_z = \sqrt{\sigma_{z_r}^2 + \sigma_{z_c}^2}$. The result is given in Tab. 3.

We will now compare the results from the three stability groups displayed in Tab. 3. We then multiply all the σ_z-values for $\lambda = 1.55$ with the constant factor 1.75 and all the σ_z-values for $\lambda = 2.4$ with the constant 5.85. The points so obtained are plotted in a log-log representation in Fig. 16. As is clearly seen from the figure, the three points for a given distance fall very close to each other. This means in mathematical language that

$$\sigma_z(x, s) = \sigma_{z_a}(x) \cdot f(s). \tag{22}$$

The relations $(\sigma_z)_{\lambda=1.55} = \sigma_{z_a}/1.75$ and $(\sigma_z)_{\lambda=2.4} = \sigma_{z_a}/5.85$ suggest the following relation (cf. eq. (22)):

$$f(s) = \frac{1}{1 + 1.9 \cdot 10^{-2} \cdot s}. \tag{23}$$

The experiments available from Ågesta are of course not enough to prove strictly that the relations (22) and (23) are the correct description of the real conditions. Especially the very few experiments performed at neutral conditions may introduce some doubt (cf. Fig. 15). But the experiments from Studsvik, the 87 m-level as well as the 24 m-level, give a stability function for σ_z, eq. (15), which is clearly closely related to eq. (23). In fact the Studsvik-equation (15) differs only from the Ågesta-equation (eq. (22) and (23)) in the presence of the function $b = b(x)$. In part IV of this paper it is shown that this latter function is produced by the topographical discontinuity in Studsvik.

Part II. A general formula for dispersion from an elevated source as a function of stability and of source height above the ground

In this part it will be shown how the experimental results from Studsvik and Ågesta presented in part I of this paper, can be used to test a general formula that describes how the vertical standard deviation of matter varies with stability and with source height above ground. First we will discuss how the vertical standard deviation at neutral stability, σ_{z_a} varies with the distance from the source.

The form for σ_{z_a} and the Lagrangian correlation as given by the Studsvik- and Ågesta experiments

We begin with the Studsvik-material, 87 m level, because this material is much more extensive (cf. p. 211) than the Ågesta-material.

On p. 217 computed σ_{z_a}-values for the 87 m level in Studsvik are listed. These values are only slightly greater than the σ_z-values for $\lambda = 0.3$ which are plotted in Fig. 9. The curve for neutral stability thus follows very closely the curve for $\lambda = 0.3$ in Fig. 9. The slope of this curve is seen to vary monotonically from about 1.0 for small x to 0.5 for great x. This suggests that the field of turbulence at near neutral stability might be at least approximately homogeneous, so that Taylor's formula can be used (Taylor, 1921):

$$\sigma_z^2 = 2\dot{w}^2 \int_0^t (t-\xi) R_L(\xi)\, d\xi \tag{24}$$

where $\dot{w}^2 = \overline{w'^2}$ and $R_L(\xi)$ is the Lagrangian correlation of the vertical velocity component.

We suppose $R_L(\xi)$ to be of the very simple form

$$R_L = e^{-a_0 \bar{u} \xi} = e^{-a_0 x}. \tag{25}$$

Eq. (24) and (25) then give:

$$\sigma_{z_a} = \frac{\dot{w}_a}{\bar{u}_a} \frac{1}{a_0} \sqrt{2(e^{-a_0 x} + a_0 x - 1)}. \tag{26}$$

For small x this formula gives:

$$\lim_{x\to 0} \frac{\sigma_{z_a}}{x} = \frac{\dot{w}_a}{\bar{u}_a} \tag{27}$$

and for great x:

$$\lim_{x\to\infty} \frac{\sigma_{z_a}}{\sqrt{x}} = \frac{\dot{w}_a}{\bar{u}_a} \sqrt{\frac{2}{a_0}}. \tag{28}$$

From eq. (27) and (28) we have

$$a_0 = \left(\frac{\sigma_z}{x}\right)^2_{x\to 0} \cdot 2 \left(\frac{x}{\sigma_z^2}\right)_{x\to\infty}. \tag{29}$$

Fig. 9 gives $\quad a_0 = 6.6 \cdot 10^{-3}$

$$\frac{\dot{w}_a}{\bar{u}_a} = 7.9 \cdot 10^{-2}.$$

σ_{z_a} has been computed from eq. (26) with the parameters given above. The result is displayed here (column two) together with the corresponding values computed directly from Tab. 2 and eq. (15) (first column):

x	σ_{z_a}	σ_{z_a} (fr. eq. (26))
100	7.18	7.15
250	15.4	15.5
500	25.5	25.8
1000	40.1	40.1
2000	60.2	59.5
4000	84.0	85.0

The extremely good agreement may of course to some extent be fortuitous, because the first column values are derived from the σ_z-values in Tab. 2 which in turn are all derived from best fit curves drawn by hand (cf. Fig. 4 and Fig. 8). But there seems to be no reason to doubt the main result, namely the usefulness of eq. (26), at least as a working formula.

For Ågesta (50 m level) we found good reasons to set forth the following formula (cf. p. 220):

$$\sigma_z(x,s) = \sigma_{z_a}(x) \cdot f(s). \tag{22}$$

In Fig. 16 the quantity $\sigma_z(x,s)/f(s)$ has been plotted from the experimental results (in the way described on p. 220) for three different stabilities. The curve drawn which is seen to fit the experimental data very closely is

$$\sigma_{z_a} = 0.11 \frac{100}{1.2} \sqrt{2(e^{-1.2\cdot 10^{-2} x} + 1.2 \cdot 10^{-2} x - 1)}. \tag{30}$$

Thus the Ågesta-data also strongly support the analytical form, eq. (26).

PASQUILL (1962*b*) has shown, that the function $\sigma_z = \sigma_z(t)$ is not very sensitive as to the exact form of R_L, if only the "Lagrangian scale of turbulence",

$$t_L = \int_0^\infty R_L(\xi)\,d\xi$$

and $\dot{w}$ are known (see his Chapter 3.5). As pointed out above the basis for the acceptance of the exact analytical form (26) is not very firm. Hence, especially when taking into account PASQUILL's abovementioned remarks, it is by no means proved that the Lagrangian correlation function has the exact form,

$$R_L = e^{-a_0 x}. \tag{25}$$

But as actual measurements of R_L are in fact almost missing, it may be of some interest to discuss the result in more detail.

INOUE (1952) has presented theoretical evidence in favour of the form (25). He presents the Lagrangian correlation in the following form:

$$R_L(\xi) = \exp\,(-\xi/\tau_0) \tag{31}$$

where ξ represents time as before. τ_0 is defined by INOUE as "the life time of the largest eddies". For vertical diffusion the following relation is claimed by INOUE to be true:

$$\tau_0 \sim \frac{z}{\dot{w}}, \text{ where } \dot{w} = \sqrt{\overline{w'^2}} \text{ as before}$$

and z is height above ground. But, as shown by many authors (PANOFSKY & MCCORMICK, 1960; MONIN, 1962; MUNN, 1961; PASQUILL, 1962*c*, etc.),

$$\dot{w}_a/\bar{u}_a = \text{const.}$$

at a given height above ground. We can then write (31):

$$R_L = \exp\left(\frac{-\dot{w}_a \alpha}{z\bar{u}_a} x\right) = e^{-a_0 x} \tag{31 a}$$

which is formally identical with eq. (25). But we can go a step further. As shown by BATCHELOR (1949)

$$\lim_{t\to\infty} \tfrac{1}{2}\frac{d\sigma_z^2}{dt} = K_p \tag{32}$$

where K_p is the coefficient of eddy exchange of matter. For the coefficient of eddy exchange of momentum we have for neutral stability in the surface layer:

$$l_a \dot{w}_a = K_a, \tag{33}$$

(cf. for instance LETTAU, 1952), l_a being the mixing length for neutral stability, and $\dot{w}_a$ having the same meaning as above.

We write
$$\frac{K_{p_a}}{K_a} = N_{p_a} \tag{34}$$

and have, from eq. (26), (32), (33) and (34):

$$N_{p_a} \dot{w}_a l_a = \frac{\dot{w}_a^2}{\bar{u}_a^2}\frac{\bar{u}_a}{a_0},$$

that is
$$a_0(z) = \frac{\dot{w}_a}{\bar{u}_a l_a N_{p_a}}. \tag{35}$$

Observing that $l_a \sim z$ in the surface layer we note the complete agreement with INOUE's result, eq. (31a). There is one point in INOUE's treatment that deserves some further discussion.

Firstly the form $R_L = e^{-a_0 x}$ can be shown (cf. BATCHELOR, 1959) to be inconsistent for very small x where the relation $dR_L/dx = 0$ must hold. INOUE meets this objection by pointing out that in his derivation of the Lagrangian spectral function which, by means of a Fourier integral transform leads to eq. (31) he does not consider the KOLMOGOROFF dissipation range of the very high frequencies. But because this range is restricted to eddies the dimensions of which is measured in millimetres or centimetres the asymptotic form (25) is surely applicable already a few metres from the source.

The general equation for the 87 m level in Studsvik and the 50 m level in Ågesta

Combining eq. (15) and (26) we have the following equation for the 87 m level in Studsvik:

$$\sigma_z(x) = \frac{\dot{w}_a}{\bar{u}_a}\frac{1}{a_0}\,\frac{\sqrt{2(e^{-a_0 x} + a_0 x - 1)}}{1 + b(x)}\left[\frac{1}{1+as} + b(x)\right]. \tag{36}$$

For small x we have

$$\lim_{x\to 0}\frac{\sigma_z}{x}=\frac{\dot{w}_a}{\bar{u}_a}\frac{1}{1+b_0}\left[\frac{1}{1+as}+b_0\right]. \qquad (37)$$

Especially for $s=0$

$$\lim_{x\to 0}\frac{\sigma_{z_0}}{x}=\frac{\dot{w}_a}{\bar{u}_a}. \qquad (27)$$

For the 50 m level in Ågesta eqs. (62) (63) and (41) combine to (with $a=1.9\cdot 10^{-2}$):

$$\sigma_z=\frac{\dot{w}_a}{\bar{u}_a}\frac{1}{a_0}\sqrt{2(e^{-a_0 x}+a_0 x-1)}\cdot\frac{1}{1+as}. \qquad (38)$$

A very interesting conclusion can be drawn from eq. (38) namely that the Lagrangian correlation coefficient is independent of stability according to the Ågesta-experiments. This has also been suggested by INOUE (1958) who claims that the quantity $\bar{u}\tau_0$, where τ_0 is "the life time of an eddy", is independent of stability. Eq. (31) then gives:

$$R_L=\exp\left(-\frac{\xi\bar{u}}{\text{const}}\right)=\exp(-a_0 x),$$

where const. $=1/a_0$ and is independent of stability. This leads us to inquire whether eq. (38) may have a very general application. If this is the case, we wish to investigate how the different parameters introduced vary with height above the ground and with topographical characteristics.

Detailed analysis of the parameters introduced in the Ågesta-equation for σ_z

a. THE STABILITY PARAMETER

At first we inquire whether there is any theoretical support for the stability parameter introduced ($=s$, see eq. (12)), and if so, if there is any theoretical evidence for the stability factor to be of the form $1/(1+\alpha s)$.

Several authors, see for instance INOUE (1958), have tried to express the influence of stability with the aid of equations of the type:

$$\sigma=\frac{\text{const}}{1+\text{const}\cdot S}$$

where S is some stability parameter like $(\theta_1-\theta_2)/\bar{u}^2$. But there seems to be no more than one rigorous theoretical treatment of the problem, namely in a paper by LETTAU (1952). As the paper appears to be more or less overlooked, applicable parts of LETTAU's derivations will be cited here. For ease of reference, LETTAU's original notations will be used here.

q_t means the instantaneous value at time t of the quantity q.

$q=\bar{q}$ means the area mean of the quantity q.

$q^{\backprime}=q_t-\bar{q}$, instantaneous deviation of q from its mean.

$$q'=\frac{\partial q}{\partial z}$$

$$q^{\cdot}=\frac{\partial q}{\partial t}.$$

The vertical acceleration exhibited by a certain particle at time t can be written:

$$\frac{Dw_t}{Dt}=\left(\frac{Dw_t}{Dt}\right)_a+\left(\frac{Dw_t}{Dt}\right)_b, \qquad (39)$$

where $(Dw_t/Dt)_a$ is the pure mechanical acceleration.

For the potential temperature, θ of the particle we have:

$$\frac{D\grave{\theta}}{Dt}=\frac{D\theta_t}{Dt}-\frac{D\bar{\theta}}{Dt}. \qquad (40)$$

If we have a source of potential heat, $S_{\theta,t}$, we get:

$$\frac{S_{\theta,t}}{\varrho c_p}=\frac{D\theta_t}{Dt}=\theta_t^{\cdot}+w_t\theta'=\bar{\theta}^{\cdot}+w_t\bar{\theta}'+\grave{\theta}^{\cdot}+w_t\grave{\theta}'. \qquad (41)$$

But

$$\left.\begin{aligned}\frac{D\bar{\theta}}{Dt}&=\bar{\theta}^{\cdot}+w_t\bar{\theta}'\\ \frac{D\grave{\theta}}{Dt}&=\grave{\theta}^{\cdot}+w_t\grave{\theta}'\end{aligned}\right\} \qquad (42)$$

so that eq. (41) and (42) give

$$\frac{D\grave{\theta}}{Dt}=\frac{S_{\theta,t}}{\varrho c_p}-\bar{\theta}^{\cdot}-w_t\bar{\theta}'. \qquad (43)$$

We observe that $\bar{\theta}$ is an area mean, so that $\bar{\theta}^{\cdot} = \partial\bar{\theta}/\partial t$ can be different from zero.

We now multiply eq. (39) by $\dot{\theta}$ and eq. (43) by w_t, add and take mean over several particles:

$$\overline{\frac{D(w_t\dot{\theta})}{Dt}} = \overline{\dot{\theta}\left(\frac{Dw_t}{Dt}\right)_a} + \overline{\dot{\theta}\left(\frac{Dw_t}{Dt}\right)_b} + \overline{w_t \frac{S_{\theta,t}}{\varrho c_p}} - \overline{w_t\bar{\theta}^{\cdot}} - \overline{w_t^2\bar{\theta}'}. \tag{44}$$

The quantity $\overline{w_t\dot{\theta}}$ is proportional to the local eddy flux of heat. Even if there is a strong variation of this quantity with height in non-neutral conditions in the atmosphere's first hectometre, there seems to be no reason for the quantity $\overline{D(w_t\dot{\theta})/Dt}$ to be different from zero in quasi-stationary conditions. Because further $S_{\theta,t}$ and $\bar{\theta}^{\cdot}$ have no reason to be correlated to w_t, eq. (44) simplifies to

$$0 = \overline{\frac{\dot{\theta}}{\theta'}\left(\frac{Dw_t}{Dt}\right)_a} + \overline{\frac{\dot{\theta}}{\theta'}\left(\frac{Dw_t}{Dt}\right)_b} - \overline{w_t^2}. \tag{45}$$

We write for the instantaneous buoyancy acceleration

$$\left(\frac{Dw_t}{Dt}\right)_b = \text{const}_1 \frac{g\dot{\theta}}{T_m} \tag{46}$$

giving
$$\overline{\frac{\dot{\theta}}{\theta'}\left(\frac{Dw_t}{Dt}\right)_b} = \text{const}_2 \cdot g \frac{\overline{\dot{\theta}^2}}{T_m\theta'} \tag{46 a}$$

(T_m is mean temperature of the layer in question; g is the acceleration of gravity).

We now define a mixing length, l, which according to LETTAU (p. 62 in his paper) is supposed to be independent of the transported property, q.

$$l = -\frac{\sigma(q)r(V,w)}{q'}, \tag{47}$$

$\sigma(q)$ being the standard deviation of q, $r(V, w)$ being the correlation coefficient for the horizontal wind component V and the vertical component w.

Eq. (47) then gives with $q = \theta$:

$$\overline{\dot{\theta}^2} = \sigma(\theta)^2 = \left[\frac{l\theta'}{r(V,w)}\right]^2. \tag{48}$$

Eqs. (45), (46 a) and (48) then give

$$\frac{\overset{\bullet}{w}^2}{l} = \overline{\frac{\dot{\theta}}{\theta'}\frac{1}{l}\left(\frac{Dw_t}{Dt}\right)_a} + \frac{\text{const}\; gl\theta'}{r^2(V,w)T_m} \tag{49}$$

where $\overset{\bullet}{w}^2 = \overline{w_t^2}$ as before.

In the limit when $\theta' = 0$

$$\frac{\overset{\bullet}{w}^2}{l} = \frac{\overset{\bullet}{w}_a^2}{l_a} = \overline{\frac{\dot{\theta}}{\theta'}\frac{1}{l}\left(\frac{Dw_t}{Dt}\right)_a}$$

LETTAU then assumes that the quantity

$$\overline{\frac{\dot{\theta}}{\theta'}\frac{1}{l}\left(\frac{Dw_t}{Dt}\right)_a}$$

is independent of stability, so that eq. (49) transforms into

$$\frac{\overset{\bullet}{w}^2}{l} = \frac{\overset{\bullet}{w}_a^2}{l_a} + \frac{\text{const}\; gl\theta'}{r^2(V,w)\,T_m} \tag{49 a}$$

LETTAU now introduces the assumption

$$\frac{\overset{\bullet}{w}}{l} = \frac{\overset{\bullet}{w}_a}{l_a}. \tag{50}$$

Eq. (49 a) and (50) give

$$\overset{\bullet}{w} = \frac{\overset{\bullet}{w}_a}{1+\xi} \tag{51}$$

with

$$\xi = \frac{-gl_a^2\theta'}{T_m\overset{\bullet}{w}_a^2}\cdot\frac{\text{const}}{r^2(V,w)}. \tag{52}$$

LETTAU further assumes that

$$\text{const} = -r(\theta,w)\cdot r(V,w) = -N_\theta r^2(V,w). \tag{53}$$

But as will be seen later, this assumption is not in accordance with observations.

LETTAU has also introduced the following relation

$$\overset{\bullet}{w}_a^2 = V_{g,0}^2 C_a^2/c_a \tag{54}$$

$V_{g,0}$ being "the geostrophic wind speed at ground level", C_a being "the geostrophic drag coefficient for neutral stability", defined as

$$C_a = \left(\frac{\tau_0}{\varrho}\right)^{\frac{1}{2}} \Big/ V_{g,0} \tag{55}$$

$c_a = \overset{\bullet}{V}_a/\overset{\bullet}{w}_a$, so that $\tau_0/\varrho = \overset{\bullet}{V}_a\overset{\bullet}{w}_a = c_a\overset{\bullet}{w}_a^2$. LETTAU

(1959) has also studied how the quantity C_a varies with the "Surface Rossby Number" defined as

$$Ro_0 = V_{g,0}/(z_0 \cdot f)$$

where z_0 is the usual roughness length and $f = 2\omega \sin \phi$, the Coriolis parameter. The variation of C_a with Ro_0 is rather slow: when Ro_0 varies from 10^7 to 10^6 for instance, C_a changes from 0.030 to about 0.042 according to LETTAU's Fig. 3 (in his 1959 paper). For a given location, z_0 and f are constants, so that the only variation in C_a is due to the variation in $V_{g,0}$. Taking into account eq. (54) we can write eq. (52) in the following way:

$$\xi = \frac{g N_\theta l_a^2 c_a}{T_m C_a^2} \frac{\frac{\partial \theta}{\partial z}}{V_{g,0}^2} \cdot A \tag{56}$$

where

$$A = -\frac{\text{const}}{r^2(V, w) N_\theta}.$$

But our stability parameter, s, is defined by eq. (12)):

$$s = \left(\frac{\partial \theta}{\partial z} \Big/ u_f^2\right) \cdot 10^5. \tag{12}$$

Now u_f (p. 212) is for practical purposes to be considered identical with $V_{g,0}$. LETTAU's (1959) introduction that "the geostrophic wind assumes in the atmospheric boundary layer the role of the ambient speed in wind tunnel experiments, or of the maximum speed (as in the centre of a pipe) in duct flow", seems even to be in favour of changing his $V_{g,0}$ into u_f. In situations with curved isobars, for instance, u_f seems to be much more analogue to the "ambient speed in wind tunnel experiments". In cases with pronounced "low level jet" (see BLACKADAR (1957) for an exhaustive treatment) it is not quite clear which is really the relevant wind to be used in eq. (53). Eqs. (51), (56) and (12) give

$$\dot{w} = \frac{\dot{w}_a}{1 + cs}, \tag{57}$$

where c varies only slowly with u_f.

In a special study, presented as an appendix to this part, it is examined how the variance of the σ_z-values observed for the 87 m-level in Studsvik behave when σ_z is regarded as a function of ξ (see eq. (56)) and of s (thus regarding C_a as a constant). The result of this study is that the variance introduced by letting C_a be constant is about one order of magnitude smaller than the total observed variance. It is also shown that the expected error in the determination of u_f (cf. eq. (12)) accounts for most of the variance observed.

We now wish to examine the relation between LETTAU's theoretical expression (57) and our equation for $\sigma_z = \sigma_z(s)$ for Ågesta. For small x the σ_z-equation for Ågesta has the following form (cf. eq. (38)):

$$\sigma_z = \frac{\dot{w}_a}{\bar{u}_a} x \frac{1}{1 + as} = \dot{w}_a \frac{\bar{u}_s}{\bar{u}_a} t \frac{1}{1 + as} \tag{58}$$

where $\bar{u}_s$ is the wind speed at stability s and free wind u_f to which free wind $\bar{u}_a$ also refers. But from TAYLOR's formula, eq. (24) (p. 221) and LETTAU's expression, eq. (57):

$$\sigma_z = \dot{w} t = \frac{\dot{w}_a}{1 + cs} t. \tag{59}$$

From eqs. (58) and (59) we have then:

$$\dot{w}_a \frac{\bar{u}_s}{\bar{u}_a} t \frac{1}{1 + as} = \frac{\dot{w}_a t}{1 + cs},$$

or

$$\frac{\bar{u}_s}{\bar{u}_a} = \frac{1 + as}{1 + cs}. \tag{60}$$

The quantity c for the 50 m level in Ågesta has been computed in the following way:

σ_{z_r}, σ_{z_c} and σ_z were computed from the original data for *fixed t-values*. The data was treated in exactly the analogue manner as for the fixed x-value case (p. 219), which means that σ_{z_r} for three stability categories was taken from best fit curves in ($\log \sigma_{z_r}$; $\log s$)-representations for fixed t-values, and σ_{z_c} from a ($\log \sigma_{z_c}$; $\log t$)-representation. The σ_z's computed with the values thus derived and eq. (1) are displayed in Fig. 17 in a ($\log \sigma_z$; $\log t$)-representation. For small t eq. (59) can be used in the form

$$\sigma_z(t) = \frac{\sigma_{z_a}(t)}{1 + cs}. \tag{59 a}$$

At a constant time t, σ_z is not a function of stability alone but of the free wind, u_f too, because (for small x):

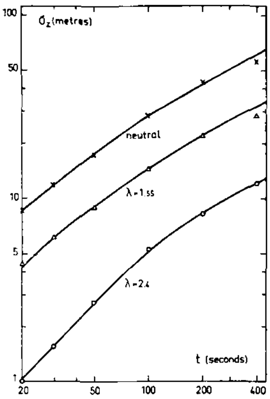

FIG. 17. Ågesta, 50 m level. σ_z as a function of time. The values are derived in an exactly analogue manner as when presented as functions of x.

$$\sigma_z = \dot{w}t = \frac{\dot{w}_a}{1+cs}t = \frac{\text{const}}{1+cs}u_f \cdot t.$$

An ideal test of the analytical form $1/(1+\alpha s)$ would then require experiments which were carried out at different stability conditions but with a common free wind. But the experiments that were used for the construction of Fig. 17 represented a fairly wide range of u_f. This of course introduced an enhanced scatter of the points in the ($\log \sigma_z - \log s$)-diagrams. But as the material showed no correlation between u_f and s, the orientation of the "point cloud" can not have been systematically changed. Fig. 17 and eq. (59a) give

$$c = 3.0 \cdot 10^{-2}.$$

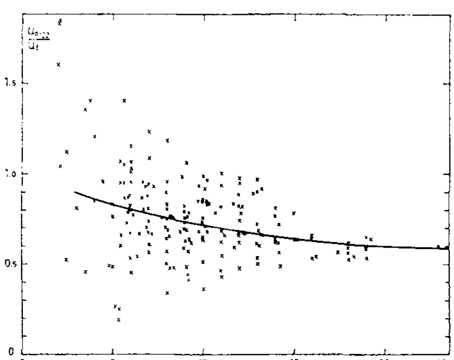

FIG. 18. Ågesta. The quotient $\bar{u}_{a122}/u_f$ as a function of the free wind, u_f (taken from Bromma, cf. p. 212). $\bar{u}_{a122}$ is hourly mean wind at 122 m level in Ågesta for near neutral stability.

b. NUMERICAL CHECKING OF LETTAU'S FORMULA

From eqs. (56), (12) and (57) we have

$$c = \frac{gN_\theta}{T_m} l_a^2 \frac{c_a}{C_a^2} \cdot 10^{-5} \cdot A. \qquad (61)$$

Having now determined c we can check this formula numerically if we can determine the parameters constituting the right member of it. Eq. (54) can be written

$$C_a = \frac{\dot{w}_a}{u_f}\sqrt{c_a}. \qquad (62)$$

The puff experiments gave (cf. p. 221):

$$\frac{\dot{w}_a}{\bar{u}_a(50)} = 0.11,$$

which with eq. (62) gives:

$$C_a = 0.11 \frac{\bar{u}_a(50)}{\bar{u}_a(122)} \cdot \frac{\bar{u}_a(122)}{u_f}\sqrt{c_a}. \qquad (63)$$

The intrusion of $\bar{u}_a(122)$ is because there is an anemometer at 122 m, so that the quotient $u_a(122)/u_f$ can be easily derived for a great number of cases. This has been done, and the points obtained have been plotted against u_f in Fig. 18. There is a great scatter of the points in the diagram as expected, remembering the crude method for determining u_f. The scatter decreases rapidly with increasing u_f as would also be expected, the error in u_f being probably almost independent of u_f itself. Group means have been derived and a curve of best fit has been drawn in Fig. 18.

The centre of gravity of the scatter diagram, Fig. 20, is situated at approximately

$$\left.\begin{aligned} \frac{\bar{u}_a(122)}{u_f} &= 0.71 \\ u_f &= 10\,ms^{-1} \end{aligned}\right\}.$$

To get further in our analysis, we must know $\bar{u}_a(50)/\bar{u}_a(122)$. Because we also need l_a in eq. (61), we must make a full analysis of the neutral wind profile in Ågesta.

During a period of about a month (mainly April 1963) six anemometers were installed on the Ågesta-mast to get a reasonably detailed wind profile. The anemometers were three of the

Lambrecht type (26 m, 72 m and 122 m) and three of the Beckman & Whitley type (5 m, 15 m and 36 m). The anemometers were calibrated in the following way, before they were installed. All the six anemometers were placed at the same level, about 1 metre above the snow covered ice of Tvären, a few hundred metres outside Studsvik. They were then run parallel for 76 hours. Hourly means were taken for the calibration, because hourly means were used for the wind profile.

It was clear from the routine wind profiles from Ågesta (122 m, 72 m and 36 m) that special wind profiles were obtained for winds from the sector 250°–290° (that is for winds perpendicular to the valley, mentioned before). For the other wind directions reasonably uniform wind profiles were obtained for near neutral conditions. Thus winds from the sector 250°–290° were excluded for the detailed study. In all c. 50 hours were left for the analysis. The mean winds derived from these 50 hours were plotted against $\log z$ in Fig. 19. The points lie all fairly close to a straight line. We use the following well known model for the profile:

$$\bar{u}(z) = \frac{\dot{V}_a}{k}\log\frac{z+z_0+d}{z_0} \tag{64}$$

$$l_a = k(z+z_0+d) \tag{65}$$

cf. for example Lettau (1952).

From Fig. 19 we derive:

$$-d = z_0 = 0.59 \text{ metres}$$

$$\frac{\dot{V}_a}{\bar{u}(50)} = 0.091.$$

But

$$c_a = \frac{\dot{V}_a}{\dot{w}_a} \qquad \text{(cf. p. 224).}$$

According to Pasquill (1962 c) the most probable value for c_a is 0.75. This means that the wind profile gives:

$$\frac{\dot{w}_a}{\bar{u}_a(50)} = 0.12$$

in excellent agreement with the result obtained entirely independently with the puff method (cf. p. 226).

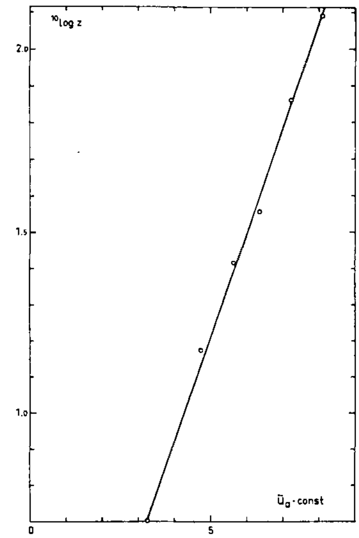

Fig. 19. Neutral wind profile for Ågesta. The line of best fit drawn satisfies $\bar{u}_a/\dot{w}_a = 4.31\ {}^{10}\log(z/0.59)$.

The wind profile can be written:

$$\bar{u}_a = 4.31\ \dot{w}_a\,{}^{10}\log\frac{z}{0.59}. \tag{66}$$

From this eq. $\bar{u}_a(122)/\bar{u}_a(50)$ is computed to be 1.20. Then C_a can be determined from eq. (63):

$$C_a = 6.4\cdot 10^{-2}\sqrt{c_a} = 5.5\cdot 10^{-2},$$

if as before $c_a = 0.75$. This C_a-value can be compared with the value obtained from Lettau's (1958) Fig. 3. With $u_f = 10$ m/s, $f = 10^{-4}$ and $z_0 = 0.6$ m one obtains $C_a = 6.0\cdot 10^{-2}$ in good agreement with our own result.

We can now examine eq. (61) for the Ågesta 50 m-level in some detail (cf. eq. (57)). The following constants are known:

c $= 3.0\cdot 10^{-2}$MKS (from the puff measurements)
g $= 9.81$ ms^{-2}
T_m $= 285$°K (a reasonable mean)
l_a $= 20$ m (from eq. (96) and $d = -z_0$)
c_a $= 0.75$ (see above)
C_a $= 5.5\cdot 10^{-2}$MKS (see above).

This gives with eq. (61):

$$N_\theta \cdot A = 0.9.$$

Because N_θ is believed not to be very different from 1.0 the above result would seem to support LETTAU's last assumption, eq. (53) which implies $A = 1.0$. But as will be seen later (p. 229) this can not be true for other levels.

The parameter N_{p_a}.

From the measurements we get (cf. Fig. 16 and eq. (30))

$$a_0 = 1.2 \cdot 10^{-2}.$$

Eq. (35),

$$a_0 = \frac{\dot{w}_a}{\bar{u}_a l_a N_{p_a}}. \tag{35}$$

From the measurements

$$\frac{\dot{w}_a}{\bar{u}_a} = 0.11; \; l_a = 20 \; m.$$

Eq. (35) and the numerical constants give $N_{p_a} = 0.5$. We repeat the definition of N_{p_a}: $N_{p_a} = K_{p_a}/K_{m_a}$. Because K_{p_a} is, for strictly homogeneous turbulence, equal to K_{z_a} (the coefficient of eddy exchange for any passive contaminant, as water vapour) it is to be expected that $N_{p_a} = 1.0$; K_{z_a} being probably equal to K_{m_a} (the coefficient of eddy exchange of momentum).

PASQUILL (1963) has shown how "the coefficient of eddy diffusivity" can be determined from a measurement of the variance of the vertical velocity at a fixed point:

$$2K = \beta T' [\sigma_w^2]_{\infty, T'}.$$

In this expression the vertical energy, σ_w^2 is averaged over the time $T' = T/\beta$, where β is a constant. The right member of the expression attains a constant value when T is sufficiently great. PASQUILL finds that during neutral conditions the value of K determined from the above relation is in accordance with the value of K_m determined from the wind profile.

In this case $N_{p_a} = 1.0$. But PASQUILL's turbulence measurements are carried out over flat agricultural countryside. From PASQUILL's equation above we see that it is the energy of the low frequencies of the vertical energy spectrum that give the highest contribution to the result, because the high frequencies are smoothed out by the averaging process. But over rough and undulatory country of the Ågesta- and Studsvik-type (observe that z_0 is about ten times greater at these two places than over flat grass covered countryside) a great part of the low frequency turbulence is probably of a wave type which in many respects has different properties than the "ordinary kind of turbulence". Thus it is not impossible to imagine a kind of "wave turbulence" which is more effective in transporting momentum than passive contaminants and so giving an N_{p_a} which is considerably less than unity.

As shown later (p. 229) the a_0-values of Studsvik, both 87 m level and 24 m level lie very close to the a_0-curve for Ågesta, described by eq. (35) and with $N_{p_a} = 0.5$. Further it is shown in part III of this paper how the Ågesta-results can be used to form a theory for ground level release, and it is also shown that the results derived in this way and with $N_{p_a} = 0.5$ give a picture which is in very good accordance with known theoretical and experimental evidence. In part III it is also demonstrated however, that ground level experiments described in the literature carried out over flat country ($z_0 < 0.1$ metre) very strongly support the use of $N_{p_a} = 1.0$.

To sum up, the parameter N_{p_a} is probably dependent on the roughness of the site, being equal to unity for flat country ($z_0 < 0.1$ metre), diminishing to at least 0.5 for very rough country ($N_{p_a} = 0.5$ for Ågesta and Studsvik where $z_0 = 0.6$ m).

c. THE VARIATION WITH HEIGHT ABOVE GROUND OF THE VARIOUS PARAMETERS PRESENTED

The σ_z-equation for the 50 m-level in Ågesta given on p. 223 has the form:

$$\sigma_z = \frac{\dot{w}_a}{\bar{u}_a} \frac{1}{a_0} \sqrt{2(e^{-a_0 x} + a_0 x - 1)} \frac{1}{1 + \bar{a}s}. \tag{38}$$

With the aid of the results already obtained it is possible to derive the z-variation of at least some of the various parameters in eq. (38) up to say $z = 75$ or 100 m with reasonable accuracy. But this is not equivalent to saying that the z-variation of σ_z is known within that same layer. Eq. (38) implies that the field of turbulence can be treated as approximately homogeneous. But the closer the point of release comes to the ground the less accurate becomes this assumption. It is not possible à priori to say what is the lowest level of applicability of eq. (38), but as the very rapid change of the turbulent variables with height is confined to say $z < 10$ m, eq. (38) is thought to give reasonable accurate results for at least $z > 20$ m. But if we know the parameters of eq. (38) for the whole range $0 < z < 100$ m, we can say that the σ_z's thus derived for any z are applicable for a hypothetical field of homogenous turbulence, characterized by the appropriate set of parameters. In part III, we will show how the σ_z's derived in this way can be used to determine realistic values for the standard deviation of vertical diffusion for release from any level in the surface layer, also from ground level.

There are four separate parameters in eq. (38) to be determined: $\dot{w}_a$, $\bar{u}_a$, a_0 and a.

The wind measurements at Ågesta showed that eq. (66) is applicable for the whole range $0 < z < 120$ m. From this equation we have immediately the relevant parameter combination $\dot{w}_a/\bar{u}_a = \dot{w}_a/\bar{u}_a(z)$. We note also that eq. (66) implies that $\dot{w}_a$ is invariant with z over the whole range.

Eq. (35) gives the formula for a_0:

$$a_0 = \frac{\dot{w}_a}{\bar{u}_a} \frac{1}{l_a} \frac{1}{N_{p_a}}, \tag{35}$$

$\dot{w}_a/\bar{u}_a$ is known from eq. (66), $l_a = 0.4\ z$ and $N_{p_a} = 0.5$. a_0 has been computed for the range $1\ \text{m} \leq z \leq 100$ m, and the result has been plotted in a log–log-diagram, Fig. 20. a_0 is seen to vary over three orders of magnitude for the range considered. The signification of this is best seen by studying the behaviour of the Lagrangian correlation function, $R_L = e^{-a_0 x}$ at different heights above ground level. This function attains the value $\frac{1}{10}$ about 500 metres from the source when $z = 100$ m, but it attains the same value already 0.5 metres from the source when $z = 1$ m.

The parameter a is closely connected with the parameter c of the LETTAU theory (cf. p. 225):

$$c = \frac{g N_\theta}{T_m} l_a^2 \frac{c_a}{C_a^2} 10^{-5} \cdot A \tag{61}$$

$$\frac{\bar{u}_s}{\bar{u}_a} = \frac{1 + as}{1 + cs}. \tag{60}$$

LETTAU (1952) assumes A to be invariant with height and equal to unity (cf. p. 228). Then $c \sim z^2$. Because further the wind profile

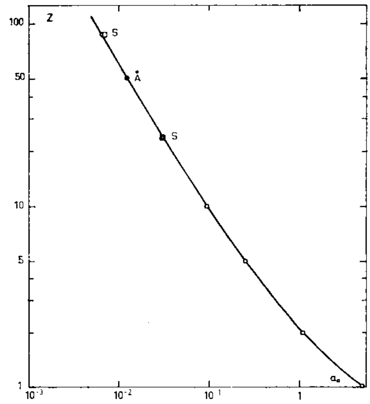

FIG. 20. The parameter a_0 as a function of height above ground. The full circle is the point derived from the puff measurements in Ågesta (50 m). The open circles are values which have been derived with the aid of eq. (35) and data for the 50 m level in Ågesta. The squares are the values obtained from the puff measurements at Studsvik (24 m and 87 m).

is linear at very great stability and logarithmic at neutral, $a = a(z)$ can be determined from eqs. (61) and (60) and the given a- and c-values for the 50 m-level. It then comes out that a varies even faster than z^2 with height. This means a very insignificant stability variation of σ_z for ground level releases. The values derived under these assumptions are in marked contrast with even the crudest estimations from continuous smoke releases at ground level, per-

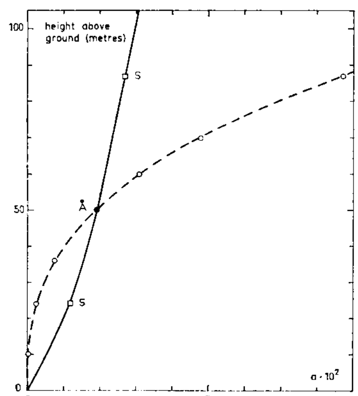

FIG. 21. The stability parameter a as a function of height. The squares are the points derived from the puff experiments in Studsvik (24 m and 87 m). The full circle is the corresponding value for Ågesta. Concerning the open circles and the hatched curve, see the text.

formed at Ågesta. These show that there is a very pronounced stability dependence of σ_z. The σ_z-data from the Prairie Grass experiments also show a marked stability dependence (cf. p. 235) which is in no way accounted for when A is supposed a constant in eq. (61).

In Fig. 21 the experimentally obtained values for a from both the Studsvik and the Ågesta experiments have been plotted. An interpolation curve for the two Studsvik values is seen to go almost straight through the Ågesta point. The curve is further extrapolated to $a = 0$ for $z = 0$, because the turbulence is probably entirely of mechanical origin very close to the ground. It seems very reasonable to assume that the full line curve drawn in Fig. 21 is a good approximation for both Ågesta and Studsvik. The hatched curve in Fig. 21 is obtained in the way just described when A is assumed unity. Many continuous smoke releases at ground level both in Studsvik and in Ågesta, show that the stability dependence of σ_z cannot be widely different at the two places (the smoke could be followed from the air up to distances of the order of 10 kilometres).

The general case. Comparison with experiments described in the literature

We will now introduce a few hypotheses of proposed general application. The only conditions to be fulfilled are:

the topography of the site is homogeneous for an appreciable distance both up-wind and down-wind;

the general meteorological conditions are stationary or only slowly changing.

The hypotheses are as follows:

1. For neutrally or stably stratified air the vertical standard deviation of matter for sampling time of the order of an hour is expressed by the formula

$$\sigma_z(x, z, s) = \frac{\dot{w}_a}{\bar{u}_a}\frac{1}{a_0}\sqrt{2(e^{-a_0 x} + a_0 x - 1)} \cdot \frac{1}{1 + as}. \tag{38}$$

The formula is immediately applicable for release from elevated sources at height z.

2. $$\frac{\bar{u}_a}{\dot{w}_a} = 4.31\ {}^{10}\log\frac{z + d + z_0}{z_0}. \tag{68}$$

Because this is simply the neutral wind profile, the region of validity is restricted to say the lowest 150 metres.

3. $$a_0 = \frac{\dot{w}_a}{\bar{u}_a}\frac{1}{l_a N_{p_a}}, \tag{35}$$

with $l_a = 0.4\ (z + d + z_0)$.
N_{p_a} is probably unity over reasonably flat country ($z_0 < 0.1$ metre, say); over rougher country N_{p_a} is probably smaller ($N_{p_a} = 0.5$ in Ågesta, where $z_0 = 0.6$ m), cf. p. 228.

4. The stability parameter

$$s = \left(\frac{\partial\theta}{\partial z}\Big/ u_f^2\right) \cdot 10^5. \tag{12}$$

5. The quantity a:

$$a = a_s(z)\frac{36 \cdot 10^{-4}}{C_a^2}. \tag{70}$$

In this equation $a_s(z)$ is the a-function obtained experimentally at Studsvik and Ågesta. The curve is represented graphically in Fig. 21.

The quantity C_a can be extracted from LETTAU's (1959) Fig. 3 or from his formulae:

$$C_a = 0.104/[{}^{10}\log(C_a R_{0_0}) - 2.24]$$

$$R_{0_0} = V_{g,0}/(z_0 \cdot f)$$

where $V_{g,0}$ is the geostrophic wind at ground level and f the Coriolis parameter.

The correctness of the hypothesis introduced can only be judged from comparison with experiments.

We begin with the neutral case.

The equation to test is

$$\sigma_z(x, z) = \frac{\dot{w}_a}{\bar{u}_a}\frac{1}{a_0}\sqrt{2(e^{-a_0 x} + a_0 x - 1)}. \tag{38}$$

To determine the parameters $(\dot{w}_a/\bar{u}_a)(z)$ and a_0, we need only know the roughness length, z_0 of the site, since $\dot{w}_a/\bar{u}_a$ is determined from the neutral wind profile

$$\frac{\bar{u}_a}{\dot{w}_a} = 4.31\ {}^{10}\log\frac{z + z_0 + d}{z_0}, \tag{68}$$

where we suppose von Karman's constant, $k = 0.4$ and $\dot{V}_a/\dot{w}_a = 0.75$ (cf. p. 227); and

$$a_0 = \frac{\dot{w}_a}{\bar{u}_a} \frac{1}{l_a N^{p_a}}, \tag{35}$$

with $l_a = 0.4(z + z_0)$. N_{p_a} is supposed to be unity.

What we need now is a set of experiments carried out at some height above ground at near neutral stability with accurately determined $\sigma_z(x)$ and with z_0 known. These requirements are met in the experiments of HAY & PASQUILL (1957). They released Lycopodium spores at a height of 500 ft, each experiment having a duration of about 30 minutes. The spores were sampled on about 20 adhesive cylinders, mounted at different heights on a balloon cable, 100, 300 and 500 metres from the source.

The roughness length, z_0 of the site is not explicitly given. But we know that the experiments were carried out at flat but somewhat rough countryside at Cardington. Then z_0 can probably not be much different from about 5 cm (cf. e.g. SUTTON 1953). If we choose $z_0 = 5$ cm eqs. (68) and (35) give $a_0 = 1.1 \cdot 10^{-3}$. Then, as seen from eq. (38) $\sigma_z(x)$ deviates from the linear form by less than about 8 % up to $x = 500$ m. This is in accordance with the result of HAY & PASQUILL who did not find any significant deviation from the linear form. The mean angular standard deviation of the experiments was 3.86°. Eq. (38) with $z_0 = 5$ cm gives this result almost exactly. Thus even if we do not know the exact z_0-value the experiments of HAY & PASQUILL must be considered to support eq. (26).

There are not many experiments to be found in the literature which can serve the purpose of testing the hypotheses for the general case, when $s > 0$. There are however some results reported by HILST & SIMPSON (1958) which refer to five releases of fluorescent pigment 185 ft above ground in stable conditions.

The proper time of sampling is not given in the paper of HILST *et al.*, but the authors claim that "there was no appreciable vertical meandering of the visible smoke plume" so we suppose that the vertical sampling is "complete" in the sense used in this paper. The temperature difference between the 300- and 100-ft level is given for each experiment as well as the average wind speed at the 200-ft level. The experimental site is characterized as "nearly flat terrain which was uniformly covered by sagebrush".

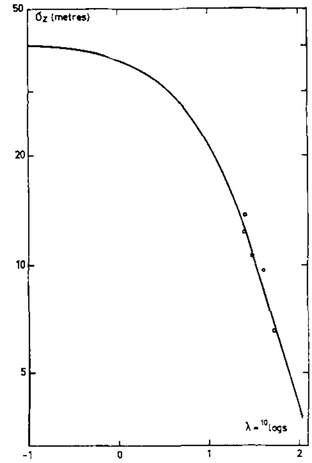

FIG. 22. σ_z-values obtained by HILST & SIMPSON (1958) for a release from a point 185 ft above ground level. Distance from the source 2500 ft. The curve drawn is $\sigma_z = 40/(1 + 9 \cdot 10^{-2} \cdot s)$. Concerning the computation of s, see the text.

Because the "free wind", u_f is not directly given for the experiments, we can only make a rather rough comparison with our theory. The stability conditions do not vary much between the experiments, so we can write

$$u_f = \alpha \bar{u}$$

where α is a constant and $\bar{u}$ the wind at 200 ft. We can then compute the stability parameter s for each experiment (eq. (12)) except for a constant factor α^{-2}. $\lambda = {}^{10}\log s$ is then determined except for an additive constant. σ_z for the distance 2500 ft from the source has been plotted on a log-scale against λ in Fig. 22. The curve drawn in the figure has been derived in the following way.

Supposing z_0 for the experimental site to be about 5 cm, σ_{z_a} has been derived with the aid of eqs. (38) (with $s = 0$), (68) and (35) (with $N_{p_a} = 1.0$). The value obtained for $x =$ 750 m (= 2500 ft) is

$$\sigma_{z_a} = 40 \text{ metres.}$$

Fig. 21 and eq. (67) give with $C_a = 3 \cdot 10^{-2}$: $a = 9 \cdot 10^{-2}$, so that with the aid of eq. (38)

$$\sigma_z = \frac{40}{1 + 9 \cdot 10^{-2} \cdot s}.$$

The experimental points fit this equation well if the constant α referred to above is made equal to 1.5. This value seems rather probable, and we conclude that the experiments of HILST *et al.* support the hypotheses 1, 5 and 6. Especially strong is the evidence for the form

$$\sigma_z = \frac{\sigma_{z_a}}{1+as},$$

that is for the hypotheses 1, because the relative configuration of the points in Fig. 22 is independent of the value of α.

To conclude, the evidence presented is in favour of the correctness of the hypotheses 1–5, which in all constitute a complete system for the determination of the vertical standard deviation of matter released from a point source at a given height above ground in specified stability conditions (not unstable stratification), given the local temperature gradient and "the free wind" and once for all the roughness length of the site. The σ_z's obtained with the formulas correspond to a sampling time of about one hour.

Next we will discuss the probable limits of validity for the equations and the degree to which they are sensitive to errors in z_0 etc.

The level of release must certainly not be below say 10 or 20 metres above the ground, because of the rapid change of the turbulent characteristics with height in the layers next to the ground. The case of ground level release will be treated in part III of this paper. The upper limit of release height is not so easily determined. The neutral wind profile for Ågesta (Fig. 19) indicates that the region may reach far beyond the 100 m level. Probably we will get a reasonably good estimation of σ_z for a release at 200 metres above ground, providing the temperature profile does not change too much with height.

The thickness of the layer of approximately constant vertical temperature gradient has also a determinative effect on the maximum distance of applicability of the equations. A certain value for the thickness of this layer gives however a very wide range of maximum distances of applicability according to whether the vertical spread is slow or fast. Roughly the equations can be considered applicable as long as σ_z is smaller than the thickness of the layer of approximately constant vertical temperature gradient. In the special case when there is an inversion present at some height above ground and the layer below the inversion is characterised by a neutral or superadiabatic temperature gradient, the concentration becomes invariant with height at distances where the computed σ_z is greater than the thickness of the "layer of good mixing". This case will be treated in some detail in part V of this paper (p. 245).

As seen from eqs. (38) and (68) $\sigma_{z_a} \propto (\log z/z_0)^{-1}$ for small distances. Eqs. (28) and (35) show that at great distances $\sigma_{z_a} \propto (\log z/z_0)^{-\frac{1}{2}}$. If we wish to determine σ_{z_a} with an error less than 10 % of its value at short distances and 5 % at long distances then z_0 must not be overestimated or underestimated by more than a factor 3.7 times its real value when $z_0 = 10^{-4}$ m, 3.0 times when $z_0 = 10^{-3}$ m, 2.3 times when $z_0 = 10^{-2}$ m, 1.9 times when $z_0 = 10^{-1}$ m and 1.5 times its real value when $z_0 = 1$ m. If we tolerate an 25 % error at short distance and 10 % at long distance, the factor of tolerance for the estimation of z_0 is respectively 25, 15, 9, 5 and 2,5 for the respective z_0-values quoted above.

An error in the estimation of N_{p_a} has no effect at all at small distances, but increases with x. At great distance $\sigma_{z_a} \propto \sqrt{N_{p_a}}$. If for instance the correct value of N_{p_a} is 0.5 but is estimated to be 1.0 the error in the determination of σ_z is none at all close to the source but grows to +40 % at great distance.

The stability parameter a is dependent of the roughness parameter z_0 as seen from eq. (70). Because the stability parameter s varies over at least a range from 0 to 10^3 an error of say a factor 1.5 in the estimation of a is of minor importance in most cases. The quantity a rises by this factor for instance when z_0 changes from 0.6 metres to 0.2 metres or from 0.2 metres to about 0.06 metres or from 0.06 metres to about 0.003 metres.

For the horizontal standard deviation the present investigation has given no such comprehensive set of formulae as for σ_z. It is however clear that the horizontal variance can be divided into two parts, one which is independent of stability and another which is dependent of stability in much the same way as is the vertical variance (see part I, p. 214). We write the total horizontal variance

$$\sigma_y^2 = \sigma_{y_1}^2 + \sigma_{y_2}^2, \tag{69}$$

with $\sigma_{y_1}^2$ being the stability independent part of the variance. Because this part is dominated by the low frequency oscillations, the Lagrangian correlation will decline rather slowly, and we will have with reasonable accuracy up to at least one or two kilometres distance:

$$\sigma_{y_1} = \frac{\sqrt{\overline{v_{30\,\mathrm{sec}}'^2}}}{\bar{u}}\, x, \tag{70}$$

where $v'_{30\,\mathrm{sec}}$ is the horizontal crosswind component averaged over 30 seconds and taken from records of a fast moving wind vane at the site.

For the stability dependent part in eq. (69) we have

$$\sigma_{y_2} = k \cdot \sigma_z \tag{71}$$

where k is probably never greater than about 2.0 or less than 1.0. Because the isotropic limit is approximately proportional to the height above ground (see for instance PRIESTLEY, 1959), the constant of proportionality, k in eq. (71) is probably continuously decreasing with height, eventually reaching the limiting value 1.0 at the top of the surface layer. When considering horizontal diffusion, the effect of the vertical wind direction shear must also be taken into account (cf. the discussion on pp. 213–215).

To determine the field of concentration for release from an elevated source when the functions $\sigma_y = \sigma_y(x)$ and $\sigma_z = \sigma_z(x)$ are known, the following well known formula will be used which supposes nearly homogeneous turbulence, Gaussian distribution of matter and no absorption of matter on the ground (cf. for instance PASQUILL, 1962*b*):

$$\chi = \frac{Q \exp(-y^2/2\sigma_y^2)}{2\pi\sigma_y\sigma_z\bar{u}(h)}\left\{\exp\left[-\frac{(z-h)^2}{2\sigma_z^2}\right] + \exp\left[-\frac{(z+h)^2}{2\sigma_z^2}\right]\right\}. \tag{72}$$

Appendix

We will examine what will be the probable error in the determination of a quantity which is supposed to be a function of ξ (see eq. (56)) when the substitution $\xi = cs$ is introduced, c being as above supposed to be constant. In Fig. 4 observations of σ_{z_r} for the 87 m level in Studsvik are plotted on a ${}^{10}\log$-scale against ${}^{10}\log s = \lambda$. A curve of best fit is drawn. We introduce the following symbols: $\eta = {}^{10}\log \sigma_{z_r}$

η_m = measured η-value.

η_t = theoretical η-value, that is the η-value for a given λ-value, taken from the curve drawn.

$\bar{\eta}$ = mean of all η_m-values.

From Fig. 4 we get:

$$\frac{\overline{(\eta_m - \eta_t)^2}}{\overline{(\eta_m - \bar{\eta})^2}} = \frac{\overline{(\delta\eta)^2}}{\overline{(\eta - \bar{\eta})^2}} = 0.1. \tag{73}$$

We now suppose that η is in fact a function of $\xi = cs = (\beta/C_a^2)s$ (cf. eq. (56)). The observed scatter of the points in Fig. 4 is then the result of:

1. errors in the determination of ξ
2. errors in the determination of σ_{z_r}.

We have:

$$\overline{(\delta\eta)^2} = \overline{\left(\frac{\partial\eta}{\partial({}^{10}\log\xi)}\right)^2}\,\overline{(\delta\,{}^{10}\log\xi)^2} + \overline{(\delta\eta_2)^2} \tag{74}$$

with

$$\overline{(\delta\,{}^{10}\log\xi)^2} = \overline{(\delta\,{}^{10}\log s)^2} + \overline{(\delta\,{}^{10}\log C_a^2)^2} \tag{75}$$

with

$$\overline{(\delta\,{}^{10}\log s)^2} = 4\overline{(\delta\,{}^{10}\log u_f)^2} + \overline{(\delta\,{}^{10}\log\theta')^2}. \tag{76}$$

From LETTAU'S (1959) Fig. 3 we have taken C_a-values for u_f ranging from 3 m/s to 17 m/s, taking $C_a = 5 \cdot 10^{-2}$ for $u_f = 10$ m/s (cf. p. 227). The C_a's are listed below together with the number of experiments carried out at the different u_f-values.

u_f	${}^{10}\log C_a^2 + 3$	Numbers of experiments
3	0.59	2
4	0.54	4
5	0.52	10
6	0.48	9
7	0.46	8
8	0.45	11
9	0.45	5
10	0.44	6
11	0.43	0
12	0.42	1
13	0.41	2
14	0.40	0
15	0.39	0
16	0.38	0
17	0.37	1

From this table it can be computed that

$$\overline{(\delta \log C_a^2)^2} = 2 \cdot 10^{-3}.$$

This gives together with Fig. 4 and eqs. (74) and (75)

$$\overline{(\delta\eta)^2_{C_a}} = \overline{\left(\frac{\partial \eta}{\partial\, ^{10}\log \xi}\right)^2 (\delta\, ^{10}\log C_a^2)^2} \simeq 10^{-3}.$$

But Fig. 4 and eq. (73) give

$$\overline{(\delta\eta)^2} \simeq 0.1\overline{(\eta - \bar{\eta})^2} \simeq 10^{-2}.$$

Thus the variance introduced by letting C_a be constant is about one order of magnitude smaller than the total observed variance.

In eq. (76) the last term on the right is small compared with the term $4\overline{(\delta\, ^{10}\log u_f)^2}$ so that

$$\overline{(\delta\, ^{10}\log s)^2} \simeq 4\overline{\left(\frac{\delta u_f}{u_f} \cdot 0.434\right)^2}.$$

The error δu_f is probably 1 or 2 m/s for $u_f = 10$ m/s, so that

$$(\delta\, ^{10}\log s)^2 \simeq 2 \cdot 10^{-2}.$$

Eqs. (85) and (86) then give

$$\overline{(\delta\eta)^2_s} = \overline{\left(\frac{\partial \eta}{\partial\, ^{10}\log \xi}\right)^2 (\delta\, ^{10}\log s)^2} \simeq 10^{-2},$$

so that the error in u_f accounts for most of the variance observed.

Part III. General formulae for ground level release

a. Determination of the vertical standard deviation

In the layers next to the ground the field of turbulence is extremely non-homogeneous. Then we cannot use the ordinary TAYLOR formula, eq. (24) for the determination of the vertical standard deviation, σ_z. But we can write down an equation which is formally identical with TAYLOR's formula but with a much more general application:

$$\sigma_z^2(x) = 2\int_0^x dx' \int_0^{x'} \overline{\frac{w}{\bar{u}}(x') \cdot \frac{w}{\bar{u}}(x'')}\, dx''. \qquad (77)$$

In the case to be considered here, $\overline{w^2}/\bar{u}^2$ is a function of the height above ground, z. The mean under the integral sign is taken over a great number of individual particle paths, some of which may traverse rather deep layers of air.

Suppose now that the particles have a GAUSSIAN distribution in the vertical at distance x_1 (the discussion to follow is in no way sensitive as to the exact form of the distribution) and a standard deviation $\sigma_z(x_1)$. Then half the particles at x_1 are below the level $z = 0.7\,\sigma_z(x_1)$ and 90 % below $z = 1.65\,\sigma_z(x_1)$. Because all the particles started at $z = 0$, almost all the particles paths up to the distance x_1 are confined to the layers below, say $z = 1.5\,\sigma_z(x_1)$.

But with the aid of eq. (38) for Ågesta we can compute $\sigma_z(x_1)$ for any height z, assuming a hypothetical field of homogeneous turbulence, characterized by the appropriate set of parameters $(\mathring{w}_a/\bar{u}_a)(z)$, $a_0(z)$ and $a(z)$ (cf. p. 230). Suppose that σ_z, derived in this way for $x = x_1$ is continuously increasing with height (cf. the example from Ågesta to be discussed below). We denote the hypothetical σ_z derived in the way just described by $\sigma_h(z, x_1)$ and the real standard deviation by $\sigma_z(x_1)$.

It is evident that σ_h for the level $z = 1.5\,\sigma_z(x_1)$ must be greater than $\sigma_z(x_1)$ because the real standard deviation $\sigma_z(x_1)$ is the integrated result of turbulent processes in the layer below

$z\,(m)$	$\sigma_h\,(m)$	$z\,(m)$	$\sigma_h\,(m)$
1	10.1	18	23.2
2	13.2	20	23.9
4	14.9	22	24.6
6	16.5	24	25.4
8	17.9	26	26.0
10	19.2	28	26.7
12	20.3	30	27.2
14	21.3	40	29.8
16	22.3		

$z = 1.5\,\sigma_z(x_1)$ as discussed above. As a working hypothesis we now assume that $\sigma_z(x_1)$ can be obtained from a computation of $\sigma_h(z, x_1)$ in the way that $\sigma_z(x_1)$ is supposed to equal the $\sigma_h(z)$-value for which holds the identity

$$0.7\,\sigma_h(z_1) \equiv z_1. \qquad (78)$$

Thus the example from Ågesta (the table) gives with eq. (78) $\sigma_h = \sigma_z = 22.0$ metres.

Now our hypotheses for the determination of σ_z for ground level release are as follows:

If the topography of the site is homogeneous for an appreciable distance both up-wind and down-wind, and if the general meteorological conditions are stationary or only slowly changing, then the vertical standard deviation of matter released from a continuous point source at ground level is determined from the formulae

$$\left.\begin{array}{l} 0.7\,\sigma_h(z_1) \equiv z_1 \\ \sigma_h(z_1) = \sigma_z(x) \end{array}\right\}. \qquad (79)$$

The function $\sigma_h = \sigma_h(z)$ is determined from the following set of formulae (cf. p. 230):

$$\sigma_h = \frac{\dot{w}_a}{\bar{u}_a}\frac{1}{a_0}\sqrt{2(e^{-a_0 x} + a_0 x - 1)}\,\frac{1}{1+as} \qquad (38)$$

$$\frac{\bar{u}_a}{\dot{w}_a} = 4.31\,{}^{10}\log\frac{z+d+z_0}{z_0} \qquad (68)$$

$$a_0 = \frac{\dot{w}_a}{\bar{u}_a}\frac{1}{l_a N_{p_a}} \qquad (35)$$

$$l_a = 0.4(z+z_0+d). \qquad (80)$$

N_{p_a} is supposed to be unity over fairly flat country (say $z_0 < 0.1$ metre); over rougher country N_{p_a} is probably smaller ($N_{p_a} = 0.5$ in Ågesta where $z_0 = 0.6$ m), (cf. p. 228).

For the determination of s and a, see p. 230.

We now turn to examine some ground level releases, presented in the literature. We begin with SUTTON's Cardington experiments of 1931 (cf. PASQUILL, 1962*b*, p. 150). These experiments give $\sigma_z = 11.1$ m as a mean for several near neutral experiments for $x = 229$ m.

With $z_0 = 5$ cm and $N_{p_a} = 1.0$ eqs. (78), (38), (68), (35) and (80) give:

$z(m)$	$0.7\sigma_h(m)$	$z(m)$	$0.7\sigma_h(m)$
1	4.0	7	7.8
2	5.0	8	8.0
3	5.8	9	8.4
4	6.4	10	8.5
5	7.0	15	9.6
6	7.3		

Applying eq. (79) gives $\sigma_z = 11.4$ m, in good agreement with the measurements. If N_{p_a} is supposed to have the same value as in Studsvik and Ågesta, that is 0.5, σ_z is computed to equal 5.0 metres instead.

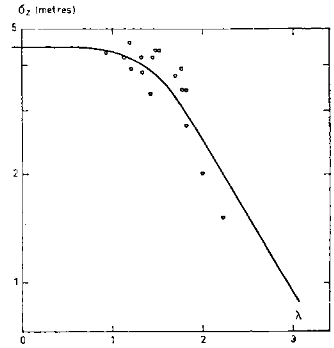

FIG. 23. Comparison between data obtained experimentally from the "Project Prairie Grass" for $x = 100$ m: the circles, and theoretically with the aid of eqs. (38), (79), (68), (35), (12) and (67): the curve.

In the "Project Prairie Grass" vertical sampling was performed at $x = 100$ m at different levels in 6 masts (see BARAD & HAUGEN, 1958; CRAMER, RECORD & VAUGHAN, 1958; and BARAD & HAUGEN, 1959). At O'Neill $z_0 = 0.9$ cm. The mean σ_z for near neutral cases is 4.5 metres. Supposing $N_{p_a} = 1.0$ as before, the eqs. (35), (68), (38) and (79) give exactly that result. Supposing again $N_{p_a} = 0.5$ gives $\sigma_{z_a} = 1.8$ metres.

We can thus say that our hypotheses above are very well supported by the experiments described in the literature for the near neutral cases.

Experiments performed at stable conditions and with all data necessary for examining our hypotheses seem only to be available in the Prairie Grass experiments.

BARAD & HAUGEN (1959) have computed σ_z for $x = 100$ m for those Prairie Grass data "with Gaussian arcwise concentration distribution". From BARAD & HAUGEN (1958) u_f and $\partial\theta/\partial z$ (cf. eq. 12) can be obtained for each of the experiments. u_f has been supposed equal to the wind at the 500 m level. For the computation of $\partial\theta/\partial z$ measurements of the temperature at 16 m and 0.5 m above ground have been used. In Fig. 23 ${}^{10}\log\sigma_z$ is plotted against $\lambda = {}^{10}\log s$. The curve drawn has been obtained with the aid of eqs. (38), (79), (68), (35), (12) and (67), the only parameter given being $z_0 = 0.9$ cm. There is some scatter of the points round the curve, but on the whole the measured data fit the theoretical curve quite well.

b. The field of concentration due to a ground level release

We assume the following form for the field of concentration with continuous ground level point release:

$$\chi = \frac{Q}{2\sqrt{\pi} I \sigma_z \sigma_y \bar{u}_{36}} \exp\left[-\frac{y^2}{2\sigma_y^2} - \frac{z^2}{2\sigma_z^2}\right], \quad (81)$$

where I is a function of x, and is obtained from the equation of continuity:

$$Q = \int_{-\infty}^{+\infty} \exp\left(-\frac{y^2}{2\sigma_y^2}\right) dy \int_0^{\infty} \frac{\bar{u}(z)}{\bar{u}_{36}} \frac{Q}{2\sqrt{\pi}} \cdot \frac{\exp[-z^2/2\sigma_z^2]}{\sigma_y \sigma_z \cdot I} dz,$$

$$I = \int_0^{\infty} \frac{\bar{u}(z)}{\bar{u}_{36}} \frac{1}{\sqrt{2}\sigma_z} \exp\left[-z^2/2\sigma_z^2\right] dz. \quad (82)$$

$\bar{u}_{36}$ is the mean wind at the 36 m level which was chosen here because it is an anemometer level in Ågesta, but of course any suitable reference level could be used. The eq. (81) presumes that the distribution of matter is Gaussian both in the horizontal and the vertical. The exact form of the vertical distribution is not known with certainty, but as pointed out by PASQUILL (1962*b*), his page 189, the concentration profile up to at least $z = 2\sigma_z$ is rather insignificantly changed, when the exponent s in

$$\chi \sim \exp\left[-\left(\frac{\Gamma(3/s)}{\Gamma(1/s)}\right)^{\frac{s}{2}} \left(\frac{z}{\sigma_z}\right)^s\right]$$

attains values from 1.0 to 2.5.

σ_z has been computed for Ågesta for the neutral case with the aid of eqs. (35), (68), (38) and (79). The result is presented in Table 4. To determine the quantity $I = I(x)$, the wind profile must be known. For the neutral case, this is given by eq. (66). The integration of eq. (82) is then performed numerically for the different distances (see Table 4).

The way to compute σ_y is rather tentative. We write

$$\sigma_y^2 = \sigma_{y_1}^2 + \sigma_{y_2}^2. \quad (69)$$

Here $\sigma_{y_1}^2$ is the stability independent part of the variance. This is supposed to be invariant with height, because it is mainly due to the low frequency oscillations which come out as a turning of the "mean wind" over deep layers. $\sigma_{y_1}^2$ is then taken to be equal to the stability independent part of σ_y^2 at $z = 50$ m, that is to σ_{yc}^2. The stability dependent part of the horizontal variance is taken as four times the vertical variance, that is $\sigma_{y_2} = 2\sigma_z$. This crude assumption is supported by the "Prairie Grass" investigations among others (see BARAD & HAUGEN, 1958). Table 4 gives an account of the σ_y's.

TABLE 4. *Computed diffusion parameters for ground level release at neutral conditions at Ågesta.*

$x\,(m)$	$\sigma_y\,(m)$	$\sigma_z\,(m)$	I
10	3.9	1.9	0.179
25	6.7	3.1	0.261
50	10.5	4.7	0.340
100	18.2	7.6	0.431
250	36.0	13.0	0.555
500	65.7	22.0	0.668
1000	116	37.8	0.790
1500	157	52.1	0.856
2000	199	66.5	0.910
4000	335	117	1.026

The quantity $((\chi/Q)\bar{u}_{36})_{\substack{y=0\\z=0}}$ has been computed with the aid of Table 4 and eq. (81) and has been plotted in Fig. 24 against x on a log–log-representation (curve labelled "neutral"). All the points (except perhaps that for $x = 10$ m) lie closely on a straight line. The slope of this line is 1.75. But this is exactly the result obtained experimentally by many authors (e.g. SUTTON, 1932; CRAMER, RECORD & VAUGHAN, 1958). SUTTON drew the conclusion from his result that

$$\left.\begin{aligned} \chi_{\substack{y=0\\z=0}} &= \frac{Q}{2\pi\sigma_y\sigma_z\bar{u}_1} \\ \sigma_y &= \frac{1}{\sqrt{2}} C_y x^{(2-n)/2} \\ \sigma_z &= \frac{1}{\sqrt{2}} C_z x^{(2-n)/2} \end{aligned}\right\}$$

where $n = 0.25$ and C_y and C_z are some constants and $\bar{u}_1$ is the mean wind at some specified level. But this is equivalent to putting I equal to a constant. From Table 4 is seen

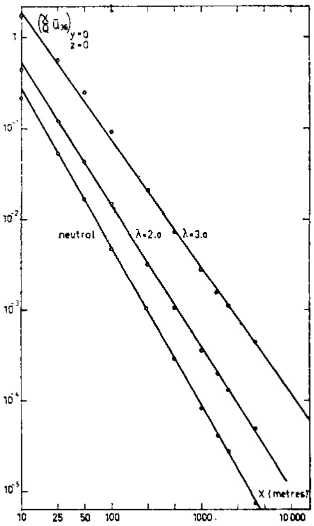

Fig. 24. Computed values for axial relative concentration, $([\chi/Q]\,\bar{u}_{36})_{\substack{y=0\\z=0}}$, for ground-level release at Ågesta for neutral stability and for $\lambda = 2.0$ and $\lambda = 3.0$.

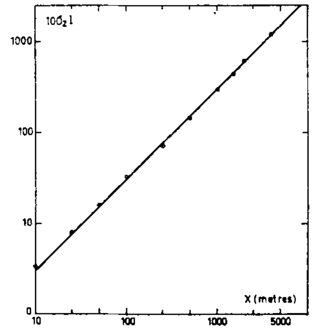

Fig. 25. The quantity $(10\,\sigma_z \cdot I)$ as a function of distance, x for ground level release at neutral stability in Ågesta. Because the concentration, χ_l, from an infinite crosswind line source at ground level is proportional to $(\sigma_z \cdot I)^{-1}$, the figure shows that $\chi_l \propto 1/x$.

that I varies by a factor of 6 from $x = 10$ m to $x = 4000$ m.

The explanation of Sutton's contradictory results is that he in fact measured the variation of χ with x and not explicitly the variation of σ_y and σ_z with x.

The concentration field from an infinite cross wind line source at ground level is obtained by integrating eq. (81) with respect to y from $-\infty$ to $+\infty$. The result is that

$$\chi_l \sim \frac{1}{\sigma_z I}. \tag{83}$$

Relevant values have been taken from Table 4 and the result has been plotted on a $(\log(\sigma_z \cdot I); \log x)$-scale, Fig. 25. The points computed lie on a straight line, the slope of which is 1.0. This means that

$$\chi_l \sim \frac{1}{x}. \tag{84}$$

This result has been predicted theoretically by Monin (1959) and obtained experimentally by Kazanskii & Monin (1957). The same value can also be inferred from the Prairie Grass data (cf. Pasquill, 1962*b*, p. 154).

It is evident that the results obtained for neutral stability in Ågesta are in excellent agreement with experiments.

We will now determine the variation of χ with distance for some stable cases for Ågesta. For simplicity we neglect the variation of $\partial\theta/\partial z$ with height. For the Ågesta case this cannot introduce very serious errors, because according to long series of observations the inversion temperature profile is known not to deviate very much from the linear form in most cases.

With $a = a(z)$ taken from the full line curve in Fig. 21, $\sigma_z(x)$ has been computed with the aid of eqs. (35), (68), (38) (see p. 230) and (79) for the stabilities $s = 100$ and $s = 1000$. The result is displayed in Table 5.

The table also gives the corresponding values for σ_y and for I. σ_y has been derived in the way described on p. 236. The quantity I has been computed with the aid of eq. (82). The quantity $\bar{u}(z)/\bar{u}_{36}$ for $s = 10^2$ and $s = 10^3$ which is necessary to know for the evaluation of eq. (82) has been derived from 250 three level wind profiles (levels: 36 m, 72 m and 122 m).

The quantity $((\chi/Q)\,\bar{u}_{36})_{\substack{y=0\\z=0}}$, has been computed with the aid of eq. (81) and Table 5. The result is plotted against x in the same figure as the neutral case (Fig. 24). As seen from the figure, the points lie on straight lines. The slope of the line for $\lambda = 2.0$ (that is $s = 10^2$) is 1.57 and for the more stable case $\lambda = 3.0$ the

TABLE 5. *Computed diffusion parameters for ground level release at Ågesta for $\lambda = 2.0$ and $\lambda = 3.0$.*

x	σ_y	I	σ_z	$^{10}\log(\sigma_y \sigma_z I)$
		$\lambda = 2.0$		
10	3.6	0.103	1.7	0.799 − 1
25	5.9	0.145	2.7	0.363
50	9.1	0.188	3.6	0.813
100	14.7	0.235	5.4	1.272
250	30.7	0.321	8.9	1.942
500	55.0	0.390	12.6	2.432
1000	94.5	0.471	17.7	2.896
1500	126	0.525	21.6	3.155
2000	156	0.572	24.7	3.343
4000	250	0.691	34.0	3.770
		$\lambda = 3.0$		
10	2.88	0.043	1.35	0.224 − 1
25	4.50	0.057	1.90	0.688 − 1
50	6.85	0.070	2.35	0.052
100	11.6	0.090	2.90	0.482
250	26.3	0.126	4.05	1.128
500	50.0	0.145	5.20	1.577
1000	88	0.177	6.50	2.007
1500	119	0.200	7.45	2.250
2000	148	0.215	8.15	2.414
4000	240	0.262	10.25	2.810

slope is 1.40. It is worth noting that a recent theoretical investigation (GIFFORD, 1962) indicates that the slope will be 1.3 for the extremely stable case.

The σ_z-values presented in Table 5 are in good qualitative agreement with observations of the continuous smoke releases in Ågesta referred to above.

To conclude, the Ågesta-results as well as results from experiments described in the literature are all in clear evidence for the system of formulae for ground level release, presented in this paper, that is for eq. (79)—to be used with eqs. (38), (68), (35) and (80) and for the eqs. (81) and (82).

In the layers next to the ground the vertical temperature gradient is often changing rapidly with height. This means strictly that when determining $\sigma_h = \sigma_h(z)$ the local gradient at height z must be taken into consideration. In most conditions however it is probably enough to use a mean vertical temperature gradient for a layer of the same order of magnitude as the relevant σ_z. The above said is true within reasonable limits only when the gradient is changing continuously with height. When there is an inversion above a neutral layer and at a height comparable to or less than the computed σ_z, this value will probably be wrong (cf. p. 250).

On p. 232 was discussed to what extent σ_z for non-ground releases is sensitive to errors in the estimation of z_0. It was found that there is a far reaching tolerance. Thus if z_0 is overestimated or underestimated by a factor 5 this would give an error to σ_{z_a} less than about 25 % if z_0 is less than about 0.1 metre. Also the stability parameter a is rather insensitive to errors in z_0. The tolerance for errors in z_0 for ground level releases is considerably smaller. If for example $z_0 = 0.9 \cdot 10^{-2}$ m $\sigma_{z_a} = 4.5$ m for $x = 100$ m. Multiplying z_0 by a factor 5 ($z_0 = 4.5 \cdot 10^{-2}$ m) gives $\sigma_{z_a} = 2.6$ metres, a change by 75 %. The σ_z-values for ground level release is also very sensitive to wrong N_{p_a}-values (cf. p. 228). In the example quoted above for $z_0 = 0.9 \cdot 10^{-2}$ m $N_{p_a} = 1.0$. Changing N_{p_a} to 0.5 gives $\sigma_{z_a} = 1.8$ m, a decrease thus by 150 %.

Part IV. Examination of the influence of a topographical discontinuity on diffusion

a. Description of the experimental results

In the preceding two parts of this paper it has been shown how the puff experiments from Ågesta formed the basis of a very general description of atmospheric diffusion. The experiments from Studsvik have also been quoted now and then. The reason why these experiments could not be taken into full account in the treatment of the general case is that there are local effects present at Studsvik which distort the picture.

Because however the Studsvik-material is so extensive (72 full experiments from the 87 m level and 18 experiments from the 24 m level), it offers an extremely good opportunity to study in a quantitative way how the "ideal" equations, presented in part II are changed when the condition of homogeneous topography is violated in a rather well defined manner.

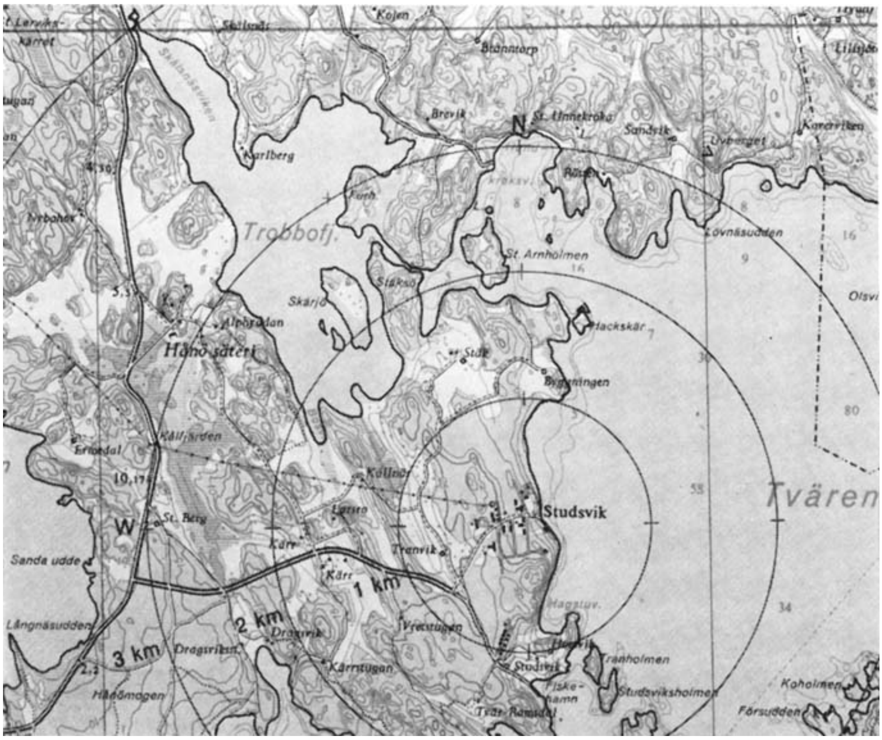

Enl. Kungl. Maj:ts beslut den 14 dec. 1962 innehar Svenska Reproduktions AB rätten till särtrycksframställning ur de officiella kartorna.

FIG. 26. Map of the Studsvik area. The chimney from which the 87 m level experiments were performed is situated at the centre of the concentric circles.

We begin with an examination of the mean trajectories of the puffs released from 87 m.

When studying the trajectories of the different puffs, one sees that the puffs travelling in landward directions have a behaviour quite different from those travelling in seaward directions. The "landward sector of winds" is sharply defined as winds from 350°, 360°, 010° ... 180° (see Fig. 26). A rather crude examination of the puffs belonging to this category revealed that they had a distinct tendency to follow the topography. To carry out a quantitative analysis of this feature cross sections were constructed from the topographical map (cf. Fig. 26) for every 10°-sector. Then from the trajectories and the cross sections the actual height of the puff centre above the ground was computed for several distances. The puffs were grouped into three stability categories, means were derived and the following result obtained:

$x\,(m)$	250	500	1000	1500	2000	2500	3000	4000
$\lambda < 1.0$	87	91	86	82	—	—	—	—
$1.0 \leq \lambda < 2.0$	88	88	86	85	85	89	—	—
$\lambda \geq 2.0$	88	83	84	89	89	93	86	83

Each value has been obtained from about 30 different trajectory values. It is clear from the table above that the mean height of the puffs above actual ground is 87 m which is equal to the height of the chimney above ground. To be sure that the mean trajectories really are streamlines at constant height above ground correlations were derived in the following way:

$$R^2 = 1 - \frac{\sum_{i=1}^{m} (\eta_i - \bar{\eta})^2}{\sum_{i=1}^{m} (z_i - \bar{z})^2}$$

where η_i is the actual height above ground of the ith puff at a certain distance; $\bar{\eta} = 87$ m;

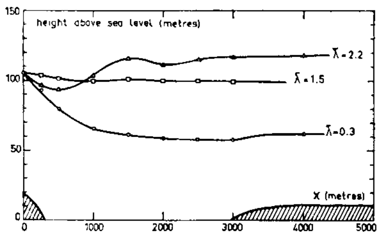

FIG. 27. Vertical section showing the mean puff trajectories for seaward wind (from 190°–340°). Each point in the figure is computed as the average position of the centre of gravity of some thirty puffs from different experiments. Legend: △ $\lambda \geq 2.0$, □ $1.0 \leq \lambda < 2.0$, ○ $\lambda < 1.0$. 87 m level in Studsvik.

z_i is the height above sea level of the terrain point over which the ith puff is situated at that very moment; $\bar{z}$ is the mean height above sea level of all the terrain points z_i. The following result was obtained for the three stability groups:

$\lambda < 1.0$	$R = 0.87$
$1.0 \leq \lambda < 2.0$	$R = 0.98$
$\lambda \geq 2.0$	$R = 0.95.$

It is thus shown with good significance that the mean trajectories are streamlines at constant height = 87 m above the underlying ground for landward trajectories. When computing σ_{z_c} this fact must be taken into account.

The seaward trajectories behave in a rather strange manner. The experiments have been divided into three stability groups and mean trajectories have been derived for each group. The result is displayed in Fig. 27. Every point is the mean of about 30 values. As seen from the Fig. 27 the near neutral and slightly unstable puffs descend to about 60 metres above the sea; the slightly stable puffs have an almost horizontal mean trajectory at about 100 metres above the sea; the most stable puffs describe a wavy motion with decreasing amplitude and come to rest about 120 metres above the sea.

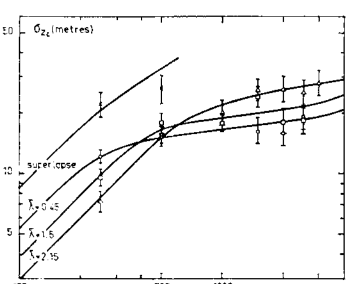

Fig. 28. 87 m level in Studsvik. σ_{z_c} for the seaward cases (wind from 190°–340°). Each point in the diagram has been computed from the formula $\sigma_{z_c} = \sqrt{\sum z_i^2 / n}$ where n is the number of puffs (usually about 20). Legend: △ $\lambda \geq 2.0$, □ $1.0 \leq \lambda < 2.0$, ○ $\lambda < 1.0$, x superlapse.

For each of the trajectories the quantity $(z - z_t)^2$ has been computed, z_t being the vertical coordinate for the relevant mean trajectory at the relevant distance. Then σ_{z_c} is computed with the aid of the formula:

$$\sigma_{z_c} = \sqrt{\frac{\sum (z_i - z_t)^2}{n}}$$

for several distances and for the three "landward" stability groups and the three "seaward" stability groups.

The result for the landward experiments is shown in Fig. 8 p. 216. Estimated errors are computed with eq. (14), p. 214 and also showed in the figure. Most probable curves are sketched by hand. As seen from the figure, σ_{z_c} is significantly stability dependent.

Fig. 28 shows the corresponding result for the seaward experiments. Also here σ_{z_c} is clearly stability dependent, but in a much more complicated manner than for the landward case. In Fig. 28 the curves cross, so that at distances of the order of a few kilometres, the most stable cases show up with the greatest σ_{z_c}-values. The 24 m puffs exhibit the same general character in their mean trajectories as do the 87 m puffs.

In part I was described how vertical turbulence (p. 217) was recorded by a light weight vane and subsequently analysed by an electronic device to give turbulence intensities directly. It was also demonstrated how the results could be related to the puff measurements from the 24 m level. The equation to be used is

$$\lim_{x \to 0} \frac{\sigma_z}{x} = \sqrt{\overline{\psi^2}} \tag{18}$$

where σ_z is the standard deviation of matter as given by the puff measurements and ψ is the angle recorded by the "Gelman instrument" (cf. p. 217).

For 87 m the result obtained was at first sight rather puzzling. Fig. 29 shows that the

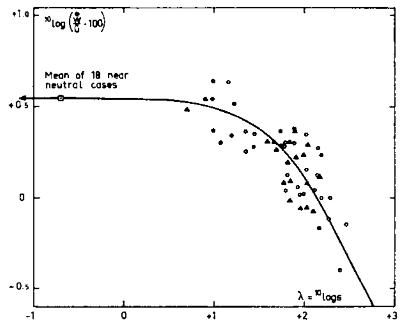

FIG. 29. Studsvik. 87 m. The quantity $(\overset{*}{w}/\bar{u})\cdot 100$ for sampling time 30 secs. The rings have been obtained from asymptotes to the curves $^{10}\log \sigma_{z_r}$ against $^{10}\log x$ (cf. Fig. 2) for each of the puff experiments. The triangles have been obtained from turbulence measurements; sampling time in this case also being 30 seconds. Each triangle represents a mean over one hour (cf. the text).

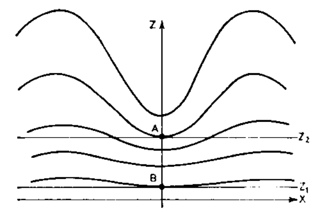

FIG. 30. A proposed model for a field of quasi stationary waves at Studsvik. A particle which describes the indicated trajectory through A exhibits a much greater amplitude than is indicated by a vertical angle measuring instrument which is fixed at A. The corresponding effect is much less pronounced at lower levels (point B).

agreement between "Gelman-results" and "puff-results" for σ_{z_r} (sampling time $\tau = 30$ sec) is good. For the longer sampling time the agreement was very bad. For near neutral stability "the Gelman-values" were scattered around the value obtained by the puff method, but for stable stratification "the Gelman-values" were systematically smaller than those obtained from eq. (37) (and hence from the puffs). This result suggests that there is a system of quasi-stationary waves present at Studsvik. A streamline pattern like that sketched in Fig. 30 would roughly explain the observed feature: an instrument at a fixed point at A would measure a vertical motion of small amplitude, whereas a particle that follows the trajectory through A would exhibit a much greater amplitude.

b. Analysis of the parameters of the Studsvik-equation for σ_z (landward case)

The σ_z-equation for the 87 m level in Studsvik, eq. (36), differs from the Ågesta-equation, eq. (38), by the presence of the function $b(x)$:

$$\sigma_z = \frac{\overset{*}{w}_a}{\bar{u}_a}\frac{1}{a_0}\cdot\frac{\sqrt{2(e^{-a_0 x}+a_0 x-1)}}{1+b(x)}\left[\frac{1}{1+as}+b(x)\right] \tag{36}$$

$$b(x) = b_1 e^{-\alpha x} + b_\infty. \tag{17}$$

We suspect that the function $b = b(x)$ is due to the presence of some system of quasi stationary waves. To begin with we will introduce a modification in eq. (45) of the LETTAU-theory (cf. p. 224):

$$\overline{\frac{\dot{\theta}}{\theta'}\left(\frac{Dw_t}{Dt}\right)_a} + \overline{\frac{\dot{\theta}}{\theta'}\left(\frac{Dw_t}{Dt}\right)_b} + \overline{\frac{\dot{\theta}}{\theta'}\left(\frac{Dw_t}{Dt}\right)_c} = \overline{w_t^2} \tag{45 a}$$

by supposing

$$\overline{\frac{\dot{\theta}}{\theta'}\left(\frac{Dw_t}{Dt}\right)_c} = \overline{w_c^2} = \overset{*}{w}{}_c^2 \tag{85}$$

where $\overline{w_c^2}$ is independent of the stability parameter. Introducing a new variable $\overset{*}{w}_1$, by the following defining equation (first two terms of eq. (45 a))

$$\overline{\frac{\dot{\theta}}{\theta'}\left(\frac{Dw_t}{Dt}\right)_a} + \overline{\frac{\dot{\theta}}{\theta'}\left(\frac{Dw_t}{Dt}\right)_b} = \overline{w_1^2} = \overset{*}{w}{}_1^2 \tag{86}$$

and supposing
$$\frac{\overset{*}{w}_1}{\overset{*}{w}_{a_1}} = \frac{l}{l_a}, \tag{50}$$

we have
$$\overset{*}{w}_1 = \frac{\overset{*}{w}_{a_1}}{1+c_1 s} \tag{87}$$

with
$$c_1 s = \frac{-\,\mathrm{const}\, g l_a^2\, \theta'}{T_m r^2(V,w)\,\overset{*}{w}{}_{a_1}^2}. \tag{52 a}$$

Introducing a constant d^2, eqs. (45 a), (85), (86) and (87) give

$$\overset{*}{w}{}^2 = \frac{\overset{*}{w}{}_a^2}{1+d^2}\left[\left(\frac{1}{1+c_1 s}\right)^2 + d^2\right], \tag{88}$$

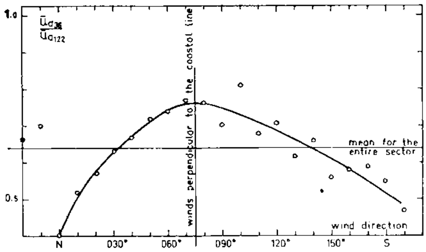

FIG. 31. The neutral wind profile in Studsvik varies systematically with wind direction.

which reduces to eq. (57), when $d^2 \to 0$. Suppose further

$$\text{const} = -N_\theta r^2(V,w) \cdot (1+d^2)^{-1} \cdot A \quad (89)$$

and eq. (52 a) gives with eq. (12):

$$c_1 = \frac{gN_\theta}{T_m} l_a^2 \frac{c_a}{C_a^2} 10^{-5} \cdot A$$

which formula is identical with eq. (61) for Ågesta.

Equations (37) and (88) give

$$\frac{\bar{u}_s}{\bar{u}_a} = \frac{\left(\sqrt{\left(\frac{1}{1+cs}\right)^2 + d^2}\right)(1+b_0)}{\sqrt{1+d^2}\left(\frac{1}{1+as} + b_0\right)}. \quad (90)$$

The parameters c and d can be determined from the puff experiments with the aid of eqs. (88) and (89), using the measurements for small distance, in which case the standard deviation is proportional to $\dot{w}$ as well as to time—cf. the corresponding derivation for the Ågesta-case, p. 225. The analysis gave the following result (which will be used in subsection e):

$$87\text{ m}: \begin{cases} c = 2 \cdot 10^{-2} \\ d^2 = 0.39 \end{cases} \qquad 24\text{ m}: \begin{cases} c = 1.43 \cdot 10^{-2} \\ d^2 = 5.6 \cdot 10^{-3} \end{cases}$$

c. Examination of some basic turbulence parameters in Studsvik

As for Ågesta we have computed $\bar{u}_a(122)/u_f$ for some hundred cases with landward winds in near neutral conditions in Studsvik. The diagram has the same over all appearance as the corresponding diagram for Ågesta, and about the same scatter of the points. For $u_f = 10$ m/s,

$$\frac{\bar{u}_a(122)}{u_f} = 0.85.$$

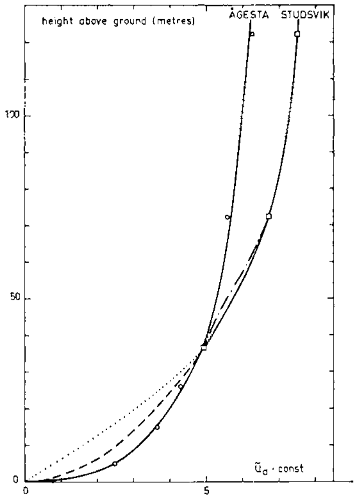

FIG. 32. Neutral wind profiles for Ågesta (circles) and Studsvik (squares) referred to the same free wind. Below 36 m the Studsvik profile is very uncertain and three possible curves have been drawn tentatively (cf. the text).

For the determination of wind profiles only three anemometers were available. These, which were all of the Lambrecht type, were installed at the levels 122 m, 72 m and 36 m above the ground as mentioned before. The anemometers were calibrated in the way described on p. 227 and besides this in a wind tunnel. According to the calibrations the relative errors of two anemometers are not likely to exceed 0.1 m/s.

The quotient $(\bar{u}_{72} - \bar{u}_{36})/(\bar{u}_{122} - \bar{u}_{36})$ was found to be significantly constant from one profile to another. The quantity $\bar{u}_{36}/\bar{u}_{122}$ on the other hand was found to vary systematically with the wind direction. As seen from fig. 31 $(\bar{u}_{36}/\bar{u}_{122})_a$ rises from 0.40 for $\varphi = 360°$ to a maximum 0.77 for $\varphi = 75°$ and then decreases again to 0.40 for $\varphi = 190°$. From the map of Studsvik, Fig. 26, it is seen that $\varphi = 75°$ corresponds to winds perpendicular to the coastal line.

Of course, the three anemometers at 36, 72 and 122 m are not sufficient to give a detailed picture of the neutral wind profile in Studsvik, especially not for the lowest decametres. Such a detailed wind profile would however be of very limited use, since the observed change of $(\bar{u}_{36}/\bar{u}_{122})_a$ with wind direction implies clearly that the wind profile is strongly dependent of the distance the wind has travelled over land. Mean winds for the three levels have been computed from all the data used in the construction of Fig. 31. The values have been plotted in Fig. 32 and a few curves have been drawn through the points. In the figure, the Ågesta neutral wind profile has also been inserted. The scale is such that the curves correspond to the same u_f. As we need the quantity $(\bar{u}_{87}/\bar{u}_{24})_a$, two extreme curves have been drawn in Fig. 32: the dotted curve which is not far from the straight line through the origin and the measured value at 36 m, and a curve which is identical with the Ågesta curve up to 36 m and then continuous into the hatched-dotted line.

We want to compute the following quantity

$$\frac{\dot{w}_{a_{24}}}{\dot{w}_{a_{87}}} = \left[\left(\frac{\dot{w}_{a_{24}}}{\bar{u}_{a_{24}}}\right) \Big/ \left(\frac{\dot{w}_{a_{87}}}{\bar{u}_{a_{87}}}\right)\right] \left(\frac{\bar{u}_{24}}{\bar{u}_{87}}\right)_a.$$

From the puff measurements we have for the level 87 m:

$$\left(\frac{\bar{u}_a}{\dot{w}_a}\right)_{87} = 12.7.$$

For the 24 m level we have from Fig. 12 (p. 218):

$$\left(\frac{\bar{u}_a}{\dot{w}_a}\right)_{24} = 12.3$$

and from the wind profiles in Fig. 32

$$1.95 \geqslant \left(\frac{\bar{u}_{87}}{\bar{u}_{24}}\right)_a \geqslant 1.65.$$

Then $$0.63 \geqslant \frac{\dot{w}_{a_{24}}}{\dot{w}_{a_{87}}} \geqslant 0.53,$$

which means that the intensity of the vertical turbulence component at neutral stability increases by about a factor two from 24 m to 87 m at Studsvik, in contrast to what is the case at an ideal site.

d. Detailed analysis of the σ_z-equation of Studsvik

It has been pointed out earlier that the topographic features of Ågesta and Studsvik are much alike (apart from the presence of the coastal line in Studsvik). But then it is very probable that the turbulence parameters change continuously with x (considering only landward winds as before) in such a way that a turbulent state is gradually attained which is not very different from that at Ågesta. We will first derive an expression for the particle variance for the non-homogeneous case, corresponding to TAYLOR's expression, eq. (24).

$$\frac{dz^2}{dt} = 2z\frac{dz}{dt} = 2z(t)\,w(t).$$

Taking means and changing the variable t into x:

$$\frac{\overline{dz^2}}{dx} = \overline{2z(x)\frac{w}{\bar{u}}(x)} = 2\int_0^x \overline{\left(\frac{w}{\bar{u}}(x)\right)\left(\frac{w}{\bar{u}}(x')\right)}dx',$$

$$\sigma_z^2(x) = 2\frac{\dot{w}^2}{\bar{u}^2}(x)\int_0^x dx' \int_0^{x'} \frac{\overline{\left(\frac{w}{\bar{u}}(x')\right)\left(\frac{w}{\bar{u}}(x'')\right)}}{\left(\frac{w}{\bar{u}}(x)\right)^2}\, dx''. \tag{91}$$

For the homogeneous case eq. (91) reduces to TAYLOR's expression, eq. (24).

For the 87 m level in Studsvik we have, according to the measurements:

$$\left(\frac{\dot{w}_a}{\bar{u}_a}\right)_{87} = 7.9 \cdot 10^{-2}.$$

For the 50 m level in Ågesta

$$\left(\frac{\dot{w}_a}{\bar{u}_a}\right)_{50} = 11 \cdot 10^{-2}.$$

From Fig. 32 we have further

$$\frac{\bar{u}_{a_{87S}}}{\bar{u}_{a_{50A}}} = 1.4$$

so that we have

$$\frac{\dot{w}_{a_{87S}}}{\dot{w}_{a_{50A}}} = 1.0.$$

From what is said above it seems probable that that Studsvik wind profile gradually approaches the Ågesta profile with increasing x. And this means also that $\dot{w}_a$ becomes constant with height up to at least 100 m. This would mean a decrease of the wind above 36 m and probably an increase in lower layers, but it would also mean a very great increase of $\dot{w}_a$ in the lower layers, because as seen from the discussion in the last sub-section, $\dot{w}_a$ at 24 m is only about one half of what it is at 87 m.

We can now give an equation for σ_z at 24 m which we had postponed obtaining (see p. 219). The turbulence measurements (Fig. 12) give

$$(\dot{w}_a/\bar{u}_a)_{24} = 8.2 \cdot 10^{-2}.$$

For small x we have from eq. (91):

$$\lim_{x\to 0} \frac{\sigma_{z_a}}{x} = \left(\frac{\dot{w}_a}{\bar{u}_a}\right)_{x=0}. \tag{92}$$

For great x the measurements (see Fig. 14) give

$$\lim_{x\to\infty} \frac{\sigma_{z_a}}{\sqrt{x}} = 0.90.$$

But for great x the field of turbulence becomes approximately homogenous, and because, for increasing x the conditions near the source is of gradually decreasing importance, eq. (28) is applicable

$$\lim_{x\to\infty} \frac{\sigma_{z_a}}{\sqrt{x}} = \left(\frac{\dot{w}_a}{\bar{u}_a}\right)_{x\to\infty} \cdot \sqrt{\frac{2}{a_0}}. \tag{28}$$

As stated above

$$\dot{w}_{a_{24}} \simeq 0.5\, w_{a_{87}}.$$

But for the 87 m level the observations indicate that $(\dot{w}_a/\bar{u}_a)$ does not vary with x. As $\bar{u}_a$ is supposed to decrease about 15 % with x, $\dot{w}_{a_{87}}$ must also decrease to the same extent. Fig. 32 indicates also that $\bar{u}_{a_{24}}$ probably increases somewhat. In fact a good fit is obtained for all x if

$$\left(\frac{\dot{w}_a}{\bar{u}_a}\right)_{24} = \left(\frac{\dot{w}_a}{\bar{u}_a}\right)_{x=0} \cdot (1.37 - 0.37\, e^{-1.35\cdot 10^{-2}x}) \tag{93}$$

and $$a_0 = 3.0 \cdot 10^{-2}.$$

The equation for the 24 m level is then from eqs. (36) and (93):

$$\sigma_z = \left(\frac{\dot{w}_a}{\bar{u}_a}\right)_{x=0} \cdot (1.37 - 0.37 \cdot e^{-1.35\cdot 10^{-2}x}) \frac{100}{3} \cdot$$

$$\cdot \sqrt{2(e^{-3\cdot 10^{-2}x} + 3 \cdot 10^{-2}x - 1)} \cdot f(s) \tag{94}$$

with (from eqs. (36), (20) and (21))

$$f(s) = \frac{\sqrt{(1 + 1.17 \cdot 10^{-2}s)} + 0.2\, e^{-4.3\cdot 10^{-2}x}}{1 + 0.2\, e^{-4.3\cdot 10^{-2}x}}. \tag{95}$$

The function (93) must not be taken too literally as being the exact function for the variation of $(\dot{w}_a/\bar{u}_a)$ with x. The main thing here is that we have found an equation for σ_z, eq. (94) that for small x equals eq. (92) and for great x equals eq. (28) with the numerical values observed and which reasonably well fits intermediate x. We will assume that for practical use the following formula is applicable for the lowest 100 metres in Studsvik

$$\sigma_z = \left(\frac{\dot{w}_a}{\bar{u}_a}\right)_{x=0} \cdot [B(z) + (1 - B(z))\, e^{-1.35\cdot 10^{-2}x}] \frac{1}{a_0} \cdot$$

$$\cdot \frac{\sqrt{2(e^{-a_0 x} + a_0 x - 1)}}{1 + b(x)} \cdot \left[\frac{1}{1 + as} + b(x)\right] \tag{96}$$

with

$$\left(\frac{\dot{w}_a}{\bar{u}_a}\right)_{x=0} \cdot B = \left(\frac{\dot{w}_a}{\bar{u}_a}\right)_{x\to\infty} = 0.85 \left(\frac{\dot{w}_a}{\bar{u}_a}(z)\right)_{\text{Agesta}}, \tag{97}$$

the correction factor 0.85 being inserted in order to make eq. (36) for the 87 m level coincide with eq. (96) for that level. This means that $\dot{w}_{a_{87}}$ decreases by some 20 % at the same time as $\bar{u}_a$ does so, making $(\dot{w}_a/\bar{u}_a)_{87}$ invariable with x, as discussed above.

We will now discuss the z-variation of the separate parameters in eq. (96).

For a_0, the values computed from the puff measurements for 24 m and 87 m coincide almost exactly with the values derived theoretically from eq. (35) for the corresponding levels at Ågesta—see Fig. 20 where the Studsvik points have been inserted as squares. It seems reasonable that the Ågesta a_0-curve (eq. (35) and Fig. 20) can be used for all levels at Studsvik.

For the quantity $a = a(z)$ the two values obtained from the puff measurements at 24 m and 87 m in Studsvik have been plotted in Fig. 21.

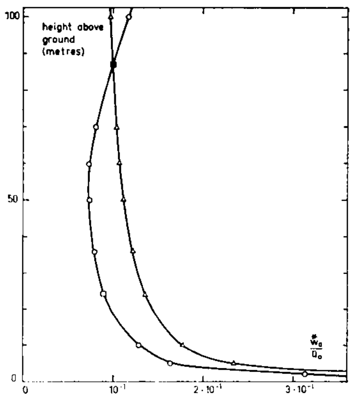

Fig. 33. $(\overset{\bullet}{w}_a/\bar{u}_a)(z)$ for Studsvik (the circles) and for Ågesta (the triangles), cf. the text.

The corresponding value for Ågesta has also been inserted. As seen from the figure, this latter point is situated on the interpolation curve for the two Studsvik-values. The result was discussed in more detail in part II.

As discussed earlier, $\overset{\bullet}{w}_{a_{24}} \simeq 0.5\, \overset{\bullet}{w}_{a_{87}}$ but we do not know anything further about the function $\overset{\bullet}{w}_a = \overset{\bullet}{w}_a(z)$. The only thing we can do is to draw some interpolation curve. What we want is a rather rough estimation of $(\overset{\bullet}{w}_a/\bar{u}_a)(z)$. Fig. 33 displays a probable curve derived from Fig. 32 and an estimated curve for $\overset{\bullet}{w}_a$. According to eqs. (96) and (97) $\overset{\bullet}{w}_a/\bar{u}_a$ will soon attain 0.85 $(\overset{\bullet}{w}_a/\bar{u}_a)_{\text{Agesta}}$. The latter curve has also been drawn in Fig. 33.

The function $b = b(z)$ can only be obtained from an interpolation curve through the points for 87 m and 24 m.

e. Theoretical examination of the local effects at Studsvik

When the air meets the coastal line, it is forced upwards at the same time as friction increases. By this process waves are excited. The amplitudes of these waves must be a maximum near the coastal line. They will then gradually die out with increasing distance from the source.

In the derivation that led to the $\overset{\bullet}{w}$-equation for Studsvik, we introduced the assumption, that the vertical turbulent energy at Studsvik by landward winds, contains a part that is independent of stability:

$$\overset{\bullet}{w}_c^2 = \frac{d^2}{1+d^2}\overset{\bullet}{w}_a^2 = \overline{\frac{\grave{\theta}}{\theta'}\left(\frac{Dw_t}{Dt}\right)_c} \tag{98}$$

(see eqs. (85) and (88)).

Suppose that the waves have sinusoidal form and that the instantaneous values of potential temperature and wind velocity θ_t and V_t are conserved during the motion. Then a particle describes the following path:

$$z = C \sin \omega t, \tag{99}$$

giving
$$w = \frac{Dz}{Dt} = C\omega \cos \omega t \tag{100}$$

and
$$\frac{Dw}{Dt} = -C\omega^2 \sin \omega t. \tag{101}$$

The mean temperature gradient is supposed to be constant $=\theta'$. The local temperature deviation, $\grave{\theta}$ caused by the wave, is then:

$$\grave{\theta} = -z\theta' = -C\theta' \sin \omega t. \tag{102}$$

We observe that the wave does not give any contribution to $r(V, w)$ and $r(\theta, w)$, (cf. the discussion on p. 224) thus giving no contribution to the term

$$\overline{\frac{\grave{\theta}}{\theta'}\left(\frac{Dw_t}{Dt}\right)_b} = r(V,w)\cdot r(\theta,w)\cdot \frac{g\overline{\grave{\theta}^2}}{\theta' T_m} A. \tag{46 a}$$

For instance, from eqs. (100) and (102):

$$r(\theta, w) = \text{const } (\overline{\grave{\theta} w}) = \text{const} \int_0^{2\pi} \sin\varphi \cos\varphi d\varphi = 0.$$

But, from eqs. (98), (101) and (102):

$$w_c^2 = \overline{\frac{\grave{\theta}}{\theta'}\left(\frac{Dw_t}{Dt}\right)_c} = \frac{C^2\omega^2}{\frac{2\pi}{\omega}} \int_0^{\frac{2\pi}{\omega}} \sin^2 \omega t dt = \frac{\omega^2 C^2}{2}. \tag{103}$$

Introducing the wave number, $\varkappa$, we have

$$\omega = \bar{u}\varkappa$$

and
$$\overset{\bullet}{w}_c^2 = \frac{C^2\bar{u}^2\varkappa^2}{2} = \frac{\overset{\bullet}{w}_a^2 d^2}{1+d^2}. \tag{104}$$

Knowing the Lagrangian correlation function, $R_L = e^{-a_0 x}$ we can use the Fourier integral transformation to get the spectral function

$$G(\varkappa) = \pi\varkappa F(\varkappa) = 2\varkappa \int_0^\infty e^{-a_0 x} \cos \varkappa x dx = \frac{2a_0\varkappa}{a_0^2 + \varkappa^2}.$$

It is seen from this function that the maximum energy of the spectrum is attained at

$$\varkappa = a_0 = 6.6 \cdot 10^{-3} m^{-1},$$

the value for the 87 m level being inserted. We suppose now that the wave energy has its maximum at about the same wave number as the spectrum as a whole. Inserting relevant numerical constants for the 87 m level in eq. (104) then gives:

$$C_{\max} \simeq 9 \text{ m},$$

a result which does not seem unreasonable.

From the equation of motion we have for the vertical component, supposing stationary conditions:

$$\overline{\frac{dw}{dt}} = \frac{\partial\overline{(uw)}}{\partial x} + \frac{\partial\overline{(vw)}}{\partial y} + \frac{\partial\overline{w^2}}{\partial z}. \tag{105}$$

At Studsvik the first two terms of the right member are very much less than the last term. Supposing near neutral conditions, we have:

$$\overline{\frac{dw_a}{dt}} = \frac{\partial \dot{w}_a^2}{\partial z}. \tag{106}$$

In Ågesta and at great distance from the source in Studsvik

$$\frac{\partial \dot{w}_a^2}{\partial z} = 0.$$

Eq. (101) gives for a certain wave:

$$\frac{dw_a}{dt} = -C\omega^2 \sin \omega t = -\omega^2 z_r, \tag{107}$$

where z_r means that the horizontal axis of the wave is situated a distance z_r from the fixed point of observation. But from reasons of continuity the wave amplitude, C must increase with height, see Fig. 30. This means that a point at a fixed height z_1 above ground is subject to waves of predominantly negative z_r. We suppose that for the 87 m level

$$\bar{z}_r \simeq \frac{-C_{\max}}{3}.$$

This and eq. (107) then gives

$$\overline{\frac{dw_t}{dt}} = \frac{C_{\max}\omega^2}{3}.$$

Taking eqs. (103) and (104) into consideration the above equation gives:

$$\overline{\left(\frac{dw_t}{dt}\right)_{87}} = \frac{\dot{w}_a^2 d^2 \cdot 2}{C_{\max}(1+d^2)3} \simeq \frac{\dot{w}_a^2}{50}.$$

From a plot of the measured $\dot{w}_a$-values at 87 m and at 24 m we can evaluate $\partial \dot{w}_a^2/\partial z$ for $z = 87$ m, and we find

$$\frac{1}{30} > \left(\frac{\partial \dot{w}_a^2}{\partial z}\right)_{87} > \frac{1}{60},$$

which shows that our supposed wave model is consistent with the turbulence characteristics recorded.

A phenomenon which is perhaps identical with our waves has been reported by HALLANGER *et cons.* (1962). They performed tracer experiments at 5 km distance from a rather stiff shore and found significant evidence for the existence of a "helix-shaped wave" of wave length 4000 yards. With $\varkappa = 6.3 \cdot 10^{-3}$ our wave system will have a wave length of about 1000 metres.

Part V. The effect of wind direction shear on the diffusion

An idealized puff contour will have the shape of an ellipse with horizontal and vertical main axes. But in practice the puff is nearly always deformed in the way shown in Fig. 34, that is, its upper parts are turned to the right, and its lower parts to the left. This effect is caused by the systematic turning of the wind with height. This turning will translate the different horizontal slices relative to each other without causing appreciable enhanced dilution unless the mixing is fairly vigorous (cf. below). As a consequence of this, the quantity $2b$ (see eq. (4b) p. 208) is equal to the maximum vertical extent of the puff and $2a$ is the horizontal width of the puff mid-way between its vertical extremities.

When computing σ_c from the trajectories of the puff centres, the mean wind direction shear interferes in a more complicated manner. Suppose in a hypothetical case that there is a vertical eddy diffusion and a mean wind direction shear but no eddy diffusion in the horizontal. Then the puff centres at a given distance from the source will all be situated on a rather thin, tilted slice. But if all these centres are projected on the $(x;y)$-plane—as they are in fact when σ_c is evaluated from a puff experiment (cf. p. 208)—then there will be a certain distribution of centres with standard deviation s_s. Return now to a real case where there is simultaneously present an horizontal eddy diffusion which at the distance in question causes a standard deviation of the particles, σ_c. The total observed variance of the distribution of centres in the y-direction at that distance is then:

$$s_{\text{tot}}^2 = \sigma_c^2 + s_s^2. \tag{108}$$

We will search for a mathematical expression for s_s assuming quasi-homogeneous turbulence. Denote by dy_s/dt the instantaneous speed in the y-direction that a certain particle attains *as a result of the systematic turning of the wind with height.* Suppose this turning to be constant with height in the layer in question and be equal to ψ radians per metre. If the particle referred to is at the height z above the level of release at a certain moment,

$$\frac{dy_s}{dt} = \frac{dx}{dt} \cdot \frac{dy_s}{dx} = \bar{u} \text{ tg } \psi z \simeq \bar{u}\psi z,$$

if we assume that the particles in question have attained the mean motion of the level z. But $dy_s^2/dt = 2y_s\, dy_s/dt$, so that taking the mean over several particles

$$\frac{\overline{dy_s^2}}{dt}(t) = 2\bar{u}\psi\overline{y_s(t)z(t)}.$$

But $$y_s(t_1) = \bar{u}\psi \int_0^{t_1} z(t_2)\,dt_2,$$ giving

$$\frac{\overline{dy_s^2}}{dt}(t) = 2\bar{u}^2\psi^2\overline{z(t)\int_0^t z(t_2)\,dt_2}$$

$$\overline{y_s^2} = 2\bar{u}^2\psi^2 \int_0^t z(t_1)\int_0^{t_1} z(t_2)\,dt_2\,dt_1.$$

But $$z(t_2) = \int_0^{t_2} w(t_3)\,dt_3,$$

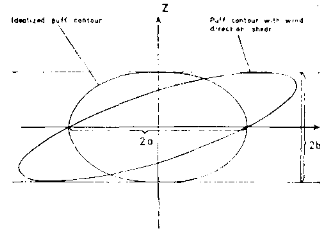

FIG. 34. The wind direction shear introduces a distortion of the puff contour, but the quantities a and b are easily measured if only the exact orientation of the puff relative to the horizon is known.

where w is the vertical velocity of the particle.

$$\overline{y_s^2(t)} = 2\bar{u}^2\psi^2 \int_0^t dt_1 \int_0^{t_1} dt_4 \int_0^{t_1} dt_2 \int_0^{t_2} \overline{w(t_4)\cdot w(t_3)}\,dt_3. \tag{109}$$

We now introduce the Lagrangian correlation, $R_L(\xi)$:

$$R_L(\xi) = \frac{\overline{w(t_3)\cdot w(t_4)}}{\overline{w^2}} \tag{110}$$

with $\xi = t_4 - t_3$. Eq. (109) becomes with eq. (110):

$$\overline{y_s^2(t)} = -2\psi^2\bar{u}^2\overline{w^2}\int_0^t dt_1 \int_0^{t_1} dt_4 \int_0^{t_1} dt_2 \int_{t_4}^{t_4-t_2} R_L(\xi)\,d\xi. \tag{111}$$

Now, according to the well known formula by TAYLOR (1921):

$$R_L(\xi) = \frac{1}{2\overline{w^2}}\frac{d^2\sigma_z^2}{d\xi^2}. \tag{112}$$

We can now solve the integral over ξ in eq. (111):

$$2\overline{w^2}\int_{t_4}^{t_4-t_2} R_L(\xi)\,d\xi = \int_{t_4}^{t_4-t_2}\frac{d^2\sigma_z^2}{d\xi^2}\,d\xi = \frac{d\sigma_z^2}{d\tau}(\tau) - \frac{d\sigma_z^2}{dt_4}(t_4),$$

where $\tau = t_4 - t_2$. Then the integral over t_2:

$$\int_0^{t_1} f(t_2)\,dt_2 = -\int_{t_4}^{t_4-t_1}\frac{d\sigma_z^2}{d\tau}\,d\tau + \frac{d\sigma_z^2}{dt_4}\int_{t_4}^{t_4-t_1} d\tau$$

$$= -[\sigma_z^2(t_4-t_1) - \sigma_z^2(t_4)] - t_1\frac{d\sigma_z^2}{dt_4}(t_4).$$

The integral over t_4:

$$\int_0^{t_1} g(t_4)\,dt_4 = -\int_{-t_1}^{0} \sigma_z^2(\tau)\,d\tau + \int_0^{t_1} \sigma_z^2(t_4)\,dt_4 - $$
$$-t_1 \int_0^{t_1} \frac{d\sigma_z^2}{dt_4}(t_4)\,dt_4 = -t_1\sigma_z^2(t_1),$$

the first two integrals cancelling out. Eq. (111) then becomes:

$$\overline{y_s^2} = \psi^2 \bar{u}^2 \int_0^t t_1 \sigma_z^2(t_1)\,dt_1 = \psi^2 \int_0^x x_1 \sigma_z^2(x_1)\,dx_1. \tag{113}$$

Thus $\overline{y_s^2}$ can be evaluated when knowing $\sigma_z = \sigma_z(t)$ or $\sigma_z = \sigma_z(x)$. A fairly good approximation is attained when assuming $\sigma_z = Cx^\alpha$. Then, from eq. (113):

$$s_s^2 = \overline{y_s^2(x)} = \frac{\psi^2 \sigma_z^2(x) \cdot x^2}{2(\alpha+1)}. \tag{114}$$

At least in fully developed homogeneous turbulence α can never be less than 0.5 or greater than 1.0 (cf. for instance BATCHELOR, 1949). This means that the denominator in eq. (114) is never less than 3.0 or greater than 4.0.

We note that the only assumption that is made in the derivation of eq. (113) (besides that the turbulence is quasi-homogeneous) is that the particles which originate at $z = 0$ have attained the mean motion of that level, z where they are at a certain moment. The correctness of this assumption can only be judged from comparison with measurements—see part I, p. 214 for further discussion.

The variance s_s^2 can be looked upon as being made up of two different parts. One is that being produced by the tilting of the axis of the cloud, the other is due to the enhanced horizontal spread of particles relative to that tilted axis. We will now search for an explicit expression for the last mentioned variance.

Now look at a certain group of particles which have that quality in common that they all pass through the line $(x_2; z_2)$, or more strictly through the parallelepiped $(x_2 + dx_2;\ z_2 + dz_2)$ at one moment in their travel from the point source at (0; 0; 0). If these particles had all traversed exactly the same path in the $(x; z)$-plane, they would of course all have crowded very close to

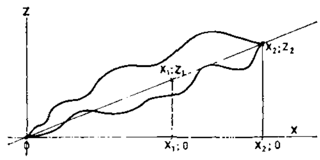

FIG. 35. Schematic diagram showing the paths of two different particles that travel from the source to the point x_2; z_2. z_1 is the mean vertical coordinate of many such particles at the distance x_1 from the source. It is supposed that (see the text):

$$z_1/z_2 = x_1/x_2$$

the point $(x_2; y_2; z_2)$ where y_2 is completely determined from the relation

$$y_2 = \bar{u}\psi \int_0^{x_2} z(x)\,dx. \tag{115}$$

But it is inherent in the statement that the vertical motion is turbulent that there is an infinite number of different paths leading from the source to $(x_2; z_2)$—see Fig. 35. Then the coordinate y_2, eq. (115) must be correspondingly spread out. We will now search for an analytical expression for the variance of the distribution of y_2, $\overline{y_d^2}$, cf. Fig. 35. Assuming Gaussian distribution the cross wind integrated concentration is:

$$\chi = \frac{Q}{\sqrt{2\pi}\,\sigma_z \bar{u}} \exp\left[-\frac{z^2}{2\sigma_z^2}\right]. \tag{116}$$

This means that the number of particles in the parallelepiped $(x_2 + dx_2;\ z_2 + dz_2)$ is proportional to:

$$d\chi_2 = \frac{Q}{\sqrt{2\pi}\,\sigma_z(x_2)\,\bar{u}} \exp\left[-\frac{z^2}{2\sigma_{z_2}^2}\right] dz_2\,dx_2. \tag{117}$$

Suppose that the particle group that constitutes $d\chi_2$ has a Gaussian distribution with standard deviation, $\sigma_L = \sigma_L(x)$ and a mean $z_1 = z_1(x)$. $\sigma_L(x)$ clearly rises from zero at the origin to a maximum and then declines to zero at x_2. The contribution from this group to the total (cross wind integrated) concentration at $(x_1; z)$ is then

$$d\chi_1 = \frac{d\chi_2}{\sqrt{2\pi}\,\sigma_L(x_1)\,\bar{u}} \exp\left[-\frac{(z-z_1)^2}{2\sigma_L^2}\right]. \tag{118}$$

But the total concentration χ_1 at $(x_1; z)$ is made up of contributions from all particles at the plain $x = x_2$ (properly speaking all particles in a slice of unit thickness). Then:

$$\chi_1(x_1, z) = \int_{-\infty}^{+\infty} \frac{Q}{2\pi\sigma_{z_2}(x_2)\,\sigma_L(x_1)} \cdot \exp\left[-\left(\frac{z_2^2}{2\sigma_{z_2}^2} + \frac{(z-z_1)^2}{2\sigma_L(x_1^2)}\right)\right] dz_2. \tag{119}$$

But this can also be written:

$$\chi_1(x_1, z) = \frac{Q}{\sqrt{2\pi}\,\sigma_z(x_1)\,\bar{u}} \exp\left[-\frac{z^2}{2\sigma_{z_1}^2}\right]. \tag{120}$$

It is very reasonable to suppose that the mean path of the particles that constitute $d\chi_2$ is the straight line between the source and $(x_2; z_2)$. That means

$$\frac{z_1}{z_2} = \frac{x_1}{x_2}. \tag{121}$$

From this, eq. (119) and eq. (120) we have for the point $(x_1; 0)$:

$$\frac{Q}{\sqrt{2\pi}\,\sigma_{z_1}\bar{u}} = \int_{-\infty}^{+\infty} \frac{Q}{2\pi\sigma_{z_2}\cdot\sigma_L\bar{u}} \cdot \exp\left[-\left(\frac{z_1^2\left(\frac{x_2}{x_1}\right)^2}{2\sigma_{z_2}^2} + \frac{z_1^2}{2\sigma_L^2}\right)\right]\cdot\left(\frac{x_2}{x_1}\right) dz_1.$$

From this follows, supposing σ_L at x_1 to be independent of z_1:

$$\sigma_L^2(x_1) = \sigma_z^2(x_1) - \sigma_z^2(x_2)\cdot\left(\frac{x_1}{x_2}\right)^2. \tag{122}$$

The same derivation that led to eq. (113) for the total "shear variance", $\overline{y_s^2}$ can be used to derive an expression for the variance relative to the tilted axis, $\overline{y_d^2}$, the only difference being that σ_z will be replaced by σ_L, so that:

$$\overline{y_d^2}(x) = \psi^2 \int_0^x x_1\,\sigma_z^2(x_1)\,dx_1 - \frac{\psi^2\sigma_{z_2}^2}{x^2}\int_0^x x_1^3\,dx_1 = \overline{y_s^2} - \frac{\psi^2\sigma_z^2(x)\cdot x^2}{4}. \tag{123}$$

If the particles travel in straight lines, $\overline{y_d^2}$ is of course zero. But if they do so, α in eq. (114) is equal to 1.0 and the denominator is 4, and we see that eq. (123) gives the right answer in this case. At a great distance from the source α is equal to 0.5 and

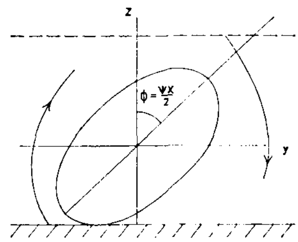

FIG. 36. The vertical wind direction shear causes the cloud axis to be tilted an angle $\phi = \psi x/2$, where ψ is the turning of the wind in radians per metre. Proximity to ground and height inversion causes modifications of the simple picture. The arrows indicate schematically the paths of reflected particles.

$$\overline{y_d^2} = \frac{\psi^2\sigma_z^2 x^2}{12} = \frac{\overline{y_s^2}}{4}. \tag{124}$$

In the case of little or no shear the equation of concentration for dispersion from a point source well removed from the ground is (assuming as before quasi-homogeneous turbulence and Gaussian distribution):

$$\chi = \frac{Q}{2\pi\sigma_y\sigma_z\bar{u}} \exp\left[-\frac{z^2}{2\sigma_z^2} - \frac{y^2}{2\sigma_y^2}\right]. \tag{125}$$

But if there is a mean wind direction shear ψ radians/m, the axis of the cloud will be tilted an angle $\varphi = \varphi(x)$—see Fig. 36.

$$\operatorname{tg}\varphi = \frac{\sqrt{\overline{y_s^2} - \overline{y_d^2}}}{\sigma_z} = \frac{\psi\sigma_z x}{2\sigma_z} = \frac{\psi x}{2} \tag{126}$$

when eq. (123) has been applied.

We now introduce the substitution

$$y' = y - z\operatorname{tg}\varphi = y - \frac{\psi z x}{2}$$

and

$$\sigma_y' = \sqrt{\sigma_y^2 + \overline{y_d^2}}$$

where σ_y is the standard deviation, due to horizontal turbulent motions only. Eq. (125) is now modified:

$$\chi = \frac{Q}{2\pi\sigma_y'\sigma_z\bar{u}} \exp\left[-\frac{z^2}{2\sigma_z^2} - \frac{\left(y - \frac{\psi z x}{2}\right)^2}{2\sigma_y'^2}\right].$$

The presence of the ground complicates the picture. Those particles reflected by the ground will be deflected towards the left in Fig. 36 as long as they are below the level of release. If the vertical mixing is halted at a certain level by an inversion, the particles "reflected" at the inversion will be transported to the right by the mean wind shear, as schematically illustrated in Fig. 36.

This means that when the mixing of the particles released is complete in the layer between the ground and the inversion, the axis of the cloud will no longer be tilted but displaced to the right if the centre of gravity of the cloud is situated lower than half way the distance between the ground and the inversion, and to the left in the contrary case. The horizontal spread of the cloud is of course highly enhanced by the process described.

PASQUILL (1962*a*) renders an account of some long distance (100 miles) tracer experiments at fairly good mixing conditions and with an inversion present at several hundred metres above ground. At some distance from the source the concentration was nearly constant with height. In spite of pronounced mean wind direction shear there was no significant tilting of the cloud axis, only a pronounced shift of the axis towards the right, in agreement with the result of the above discussion.

It is of great practical interest to find a concentration formula for the type of situation just described. It is proposed that the following formula be used ($z < H$):

$$\chi(x,y,z) = \frac{Q}{\sqrt{2\pi\bar{u}H}\sqrt{\overline{y^2}}}\exp\left[-\frac{y^2}{2\overline{y^2}}\right] \quad (127)$$

where H is the height above the ground to the inversion and (from eq. (114)):

$$\overline{y^2} = \sigma_y^2 + \overline{y_s^2} \simeq \frac{\psi^2\sigma_z^2(x)x^2}{3.3} + \sigma_y^2,$$

where σ_y^2 is the variance produced by pure turbulent diffusion.

Acknowledgements

I wish to express my gratitude to AB Atomenergi for defraying the cost of the investigation, to my chief, Dr Alf Nyberg, director of the Swedish meteorological and hydrological institute, for letting me concentrate on these problems for many years and to Prof. Gösta Liljequist at the University of Uppsala for his kind interest in my work. I appreciate very much the valuable comments given by Dr F. B. Smith and the discussions with Mr B. Bringfelt.

I will also express my sincere thanks to Mr L. E. Hæggblom and many other persons from AB Atomenergi whose enthusiastic efforts made it possible to perform the extensive experimental program, and to Mr J. Torsell, Mrs Berit Wåhlberg and several others at the Swedish meteorological and hydrological institute who performed the numerical computations.

REFERENCES

BARAD, M. L., and FUQUAY, J., 1962, The green glow diffusion program. *Geophysical Research papers*, Vol. **1**: 73, Bedford, Mass.

BARAD, M. L., and HAUGEN, D. A., 1958, Project Prairie Grass, a field program in diffusion, *Geophysical Research Papers No.* **59**, Vols. **I & II**, G.R.D., A.F.C.R.C., Bedford, Mass.

BARAD, M. L., and HAUGEN, D. A., 1959, A preliminary evaluation of Suttons's hypothesis for diffusion from a continuous source, *J. Meteor.*, **16**, p. 12.

BATCHELOR, G. K., 1949, Diffusion in a field of homogeneous turbulence, I. Eulerian analysis, *Aust. J. Sci. Res.*, **2**, p. 437.

BATCHELOR, G. K., 1950, The application of the similarity theory of turbulence to atmospheric diffusion, *Quart. J. R. Met. Soc.*, **76**, p. 133.

BATCHELOR, G. K., 1952, Diffusion in a field of homogeneous turbulence, II. The relative motion of particles, *Proc. Camb. Phil. Soc.*, **48**, p. 345.

BATCHELOR, G. K., 1959, *The theory of homogeneous turbulence*, Cambridge University Press.

BLACKADAR, A., 1957, Boundary layer wind maxima and their significance for the growth of nocturnal inversions. *Bulletin American Met. Soc.*, Vol. **38**, No. 5, p. 283.

CRAMER, H. E., RECORD, F. A., and VAUGHAN, H. C., 1958, The study of the diffusion of gases or aerosols in the lower atmosphere, *M.I.T. Department of Meteorology*, *Final Report under Contract* No. AF 19(604)-1058.

FRENKIEL, F. N., and KATZ, I., 1956, Studies of small-scale turbulent diffusion in the atmosphere, *J. Meteor.*, **13**, p. 388.

GIFFORD, F., 1957, Relative atmospheric diffusion of smoke puffs, *J. Meteor.*, **14**, p. 410.

GIFFORD, F., 1962, Diffusion in the diabatic surface layer, *J. Geophys. Research*, Vol. **67**, No. 8, p. 3207.

HALLANGER, N. L., HERD, G. R., SHORTLEY, G., and STEARMAN, R. L., 1962, Quasi-stationary waves observed in aerosol diffusion trials. *J. Atmospheric Sciences*, Vol. **19**, p. 99.

HAY, J. S., and PASQUILL, F., 1957, Diffusion from a fixed source at a height of a few hundred feet in the atmosphere. *J. Fluid Mech.*, 2, p. 299.

HAY, J. S., and PASQUILL, F., 1959, Diffusion from a continuous source in relation to the spectrum and scale of turbulence. *Atmospheric Diffusion and Air Pollution*, edited by F. N. Frenkiel and P. A. Sheppard, Advances in Geophysics, **6**, p. 345, Academic Press.

HILST, G. R., and SIMPSON, C. L., 1958, Observations of vertical diffusion rates in stable atmospheres, *J. Meteor.*, **15**, p. 125.

HÖGSTRÖM U., 1959, Utprovning av fotometrisk metod för bestämning av diffusionsparametrar, *SMHI, Met. Byrån, utredningar*, Stockholm.

INOUE, E., 1952, On the Lagrangian correlation coefficient for turbulent diffusion and its application to atmospheric diffusion phenomena, *Geophysical Research papers*, No. **19**, p. 397. AFCRC Technical Report 53-9. Bedford, Mass.

INOUE, E., 1959, The effects of thermal stratification on turbulent diffusion in the atmospheric surface layer. *Atmospheric Diffusion and Air Pollution*, edited by F. N. Frenkiel and P. A. Sheppard, Advances in Geophysics, **6**, p. 319, Academic Press.

JONES, J. I. P., and PASQUILL, F., 1959, An experimental system for directly recording statistics of the intensity of atmospheric turbulence, *Quart. J. R. Met. Soc.*, **85**, p. 225.

KAZANSKII, A. B., and MONIN, A. S., 1957, The forms of smoke trails, *Izv. Akad. Nauk. U.S.S.R.* (*Ser. Geofiz.*), No. 8, p. 1020.

KELLOGG, W. W., 1956, Diffusion of smoke in the stratosphere, *J. Meteor.*, **13**, p. 241.

LETTAU, H., 1952, The present position of selected turbulence problems in the atmospheric boundary layer, *Geophysical Research papers*, No. **19**, p. 49. AFCRC Technical Report 53-9. Bedford, Mass.

LETTAU, H., 1959, Wind profile, surface stress and geostrophic drag coefficients in the atmospheric surface layer, *Atmospheric Diffusion and Air Pollution*, edited by F. N. Frenkiel and P. A. Sheppard, Advances in Geophysics, **6**, p. 241, Academic Press.

MONIN, A. S., 1959, Smoke propagation in the surface layer of the atmosphere, *Atmospheric Diffusion and Air Pollution*, edited by F. N. Frenkiel and P. A. Sheppard, Advances in Geophysics, **6**, p. 331, Academic Press.

MONIN, A. S., 1962, Empirical data on turbulence in the surface layer of the atmosphere, *J. Geophys. Research*, Vol. **67**, No. 8, p. 3103.

MUNN, R. E., 1961, A theoretical expression for the root mean square vertical eddy fluctuation, *J. Meteor.*, **18**, p. 38.

OBUKHOV, A. M., 1962, Some specific features of atmospheric turbulence, *J. Geophys. Research*, Vol. **67**, p. 3011.

PANOFSKY, H. A., and DELAND, R. J., 1959, One-dimensional spectra of atmospheric turbulence in the lowest 100 metres, *Atmospheric Diffusion and Air Pollution*, edited by F. N. Frenkiel and P. A. Sheppard, Advances in Geophysics, **6**, p. 41, Academic Press.

PANOFSKY, H. A., and MCCORMICK, R. A., 1960, The spectrum of vertical velocity near the surface, *Quart. J. R. Met. Soc.*, **86**, p. 495.

PASQUILL, F., 1962*a*, Some observed properties of medium-scale diffusion in the atmosphere, *Quart. J. R. Met. Soc.*, 88, p. 70.

PASQUILL, F., 1962*b*, *Atmospheric diffusion*, D. van Nostrand Co. Ltd, London.

PASQUILL, F., 1962*c*, Recent broad-band spectral measurements of turbulence in the lower atmosphere, *J. Geophys. Research*, Vol. **67**, p. 3025.

PASQUILL, F., 1963, The determination of eddy diffusivity from measurements of turbulent energy. *Quart. Journ. of the Roy. Met. Soc.*, Vol. **89**, No. 379, p. 95.

PRIESTLEY, C. H. B., 1959, The isotropic limit and the microscale of turbulence, *Atmospheric Diffusion and Air pollution*, edited by F. N. Frenkiel and P. A. Sheppard, Advances in Geophysics, **6**, p. 97, Academic Press.

ROBERTS, O. F. T., 1923, The theoretical scattering of smoke in a turbulent atmosphere, *Proc. Roy. Soc.*, A, 104, p. 640.

SUTTON, O. G., 1932, A theory of eddy diffusion in the atmosphere, *Proc. Roy. Soc.*, A, **135**, p. 143.

SUTTON, O. G., 1953, Micrometeorology. McGraw Hill Books.

TAYLOR, G. I., 1921, Diffusion by continuous movements, *Proc. London Math. Soc.*, Ser. 2, 20, p. 196.